AD-A056 503 AIR FORCE INST OF TECH WRIGHT-PATTERSON AFB OHIO SCH--ETC F/G 20/5
SPATIAL FILTERING DESIGN CONSIDERATIONS FOR A LASER LINE SCANNI--ETC(U)
DEC 77 W D STRAUTMAN

UNCLASSIFIED AFIT/GEO/EE/77-6 NL

1 OF 1
AD
A056 503

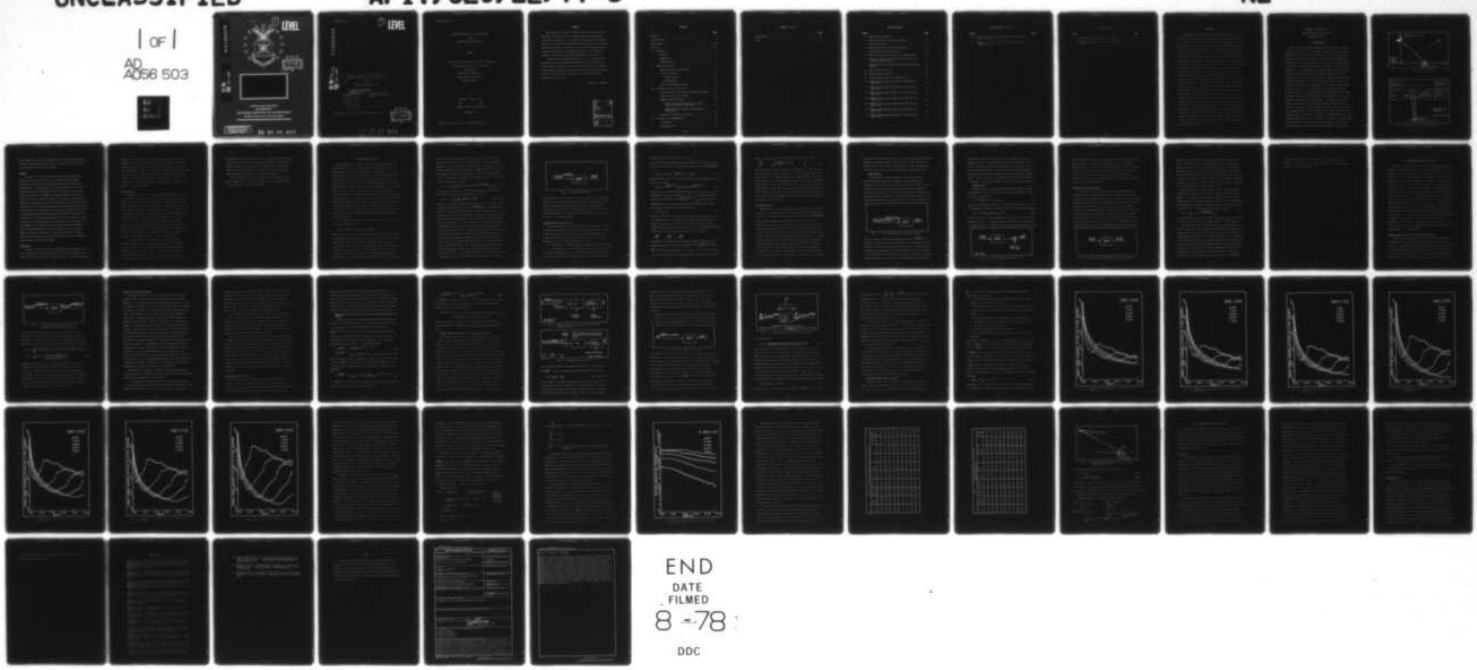

END
DATE
FILMED
8-78
DDC

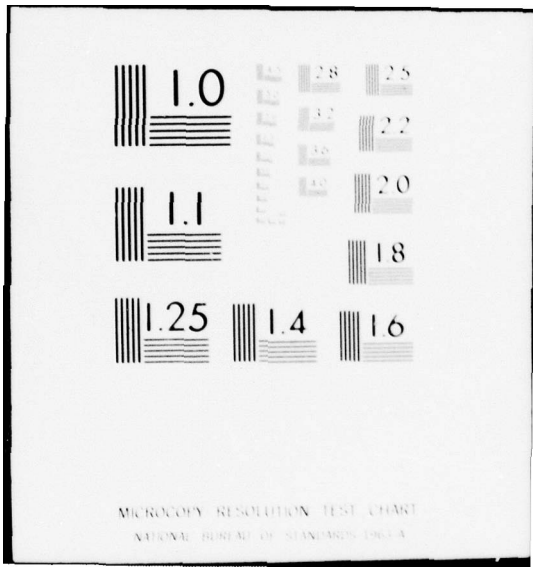
1.0
1.1
1.25
1.4
1.6
2.8
2.5
3.2
2.2
3.6
2.0
4.0
1.8
MICROCOPY RESOLUTION TEST CHART
NATIONAL BUREAU OF STANDARDS 1963-A

LEVEL II

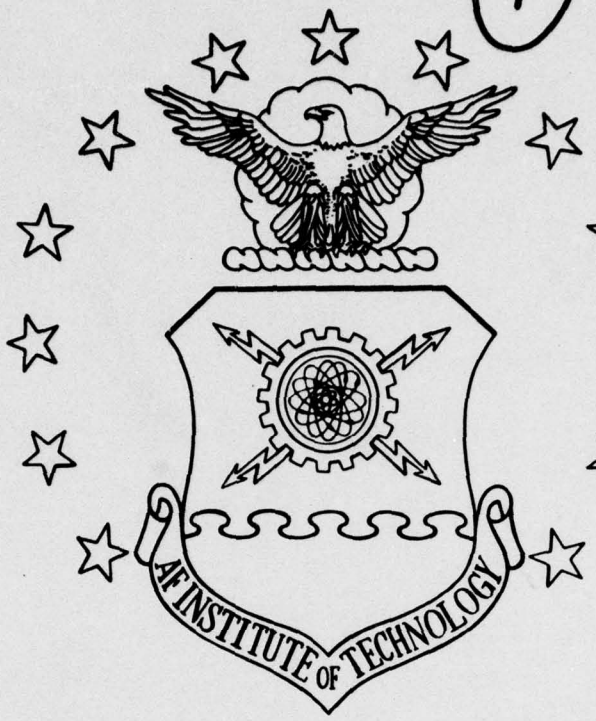

UNITED STATES AIR FORCE

AIR UNIVERSITY

AIR FORCE INSTITUTE OF TECHNOLOGY

Wright-Patterson Air Force Base, Ohio

AFIT/GEO/EE/77-6

(1) LEVEL II

AD A056503

AD No.
DDC FILE COPY

(6) SPATIAL FILTERING DESIGN CONSIDERATIONS
FOR A
LASER LINE SCANNING SENSOR.

(9) Master's THESIS,

(14) AFIT/GEO/EE/77-6

(10) William D. Strautman
USAF

(11) Dec 77

(12) 64p.

Approved for public release; distribution unlimited.

78 07 07 014

012225

AFIT/GEO/EE/77-6

SPATIAL FILTERING DESIGN CONSIDERATIONS FOR A LASER LINE SCANNING SENSOR

THESIS

Presented to the Faculty of the School of Engineering
of the Air Force Institute of Technology
Air University
in Partial Fulfillment of the
Requirements for the Degree of
Master of Science

by

William D. Strautman, B.S.
Capt USAF
Graduate Electrical Engineering

December 1977

Preface

This theoretical study was sponsored by the Air Force Avionics Laboratory in conjunction with a design study for the development of a laser line scanning sensor. The purpose of this study was to analyze the effects of spatial filtering by the finite beam size on the performance of this sensor. The distortion of the detected terrain reflectivity and range signals are modeled and analyzed. The distortion analysis is then used to describe the resolution of the sensor.

I would like to express my gratitude to Dr. B. L. Sowers for his assistance in providing background information and in reviewing this study. Special thanks goes to my thesis advisor, Capt S. R. Robinson, whose guidance and support made the completion of this thesis possible. Finally, thanks goes to my wife, Ann, for her patience during the preparation of this study.

William D. Strautman

Contents

Contents (Cont'd)

List of Figures

List of Figures (Cont'd)

List of Tables

Abstract

The performance of an airborne laser terrain mapper, which collects slant range and reflectance data simultaneously, is determined in part by the spatial filtering effects of the finite laser beam spot size. An analysis of the spatial filtering effects and the resulting distortion of the terrain profile slant range to the aircraft is made to interpret the interaction between the terrain characteristics and the resulting laser line scan information. Emphasis is placed on the range interactions. In particular, the terrain height profile is modeled as a single sinusoid in one spatial dimension with constant reflectivity. The laser transmitter is sinusoidally intensity modulated, so that the received signal is subcarrier phase modulated by the terrain height profile. This phase modulated signal is low pass filtered to represent the effects of the spatial filter. Numerical analysis is utilized to evaluate this nonlinear filtering problem and to examine the range error in terms of the maximum range height variations. The resulting mean-squared range distortion error is added to the range squared distortion error originating from the receiver noise in the Phase Locked Loop phase tracking circuit. The distortion due to spatial filtering is shown to increase with the laser modulation frequency while the errors due to detection noise decrease with frequency. Thus, the performance of the receiver can be optimized according to the terrain maximum range height variations and the desired resolution by designing the properly sized optics and choosing an optimum frequency of modulation. In addition, the general spatial filtering model is extended to evaluate the performance of a forward looking laser terrain mapper using low grazing angles.

SPATIAL FILTERING DESIGN CONSIDERATIONS FOR A LASER LINE SCANNING SENSOR

I. Introduction

The design of an airborne terrain mapping laser scanner is being studied by the Air Force. This proposed sensor would collect range and reflectivity data which could be combined and used to construct three dimensional imagery of the terrain. Some of the possible applications are referenced in an AGARD report (Ref 1). Figure 1 is a block diagram of the laser line scanning sensor which consists of the following basic components: laser illuminator, line scanner, direct detection receiver, optics train, signal processing electronics, display device, and a recording device. The line scanner is used to scan the terrain in small strips perpendicular to the aircraft's forward motion, while the line scans are incremented along the y-axis by the aircraft's forward motion as depicted in Figure 2. The beam intensity pattern as represented along the x-axis is $b(x)$, and the width of this intensity pattern along the x-axis is the beam spot size which is designated by X. The laser is intensity modulated by a periodic signal. The laser is used to illuminate the terrain with this periodic intensity modulation and this signal is detected by a direct detection receiver. Within the receiver, a particular harmonic of the periodic signal is phase tracked, and the resulting phase is compared to the phase of the transmitted signal. The phase difference between the two signals is converted to the slant range from the aircraft to the terrain spot being scanned. Since the phase used to determine the slant range is relative phase, it may contain

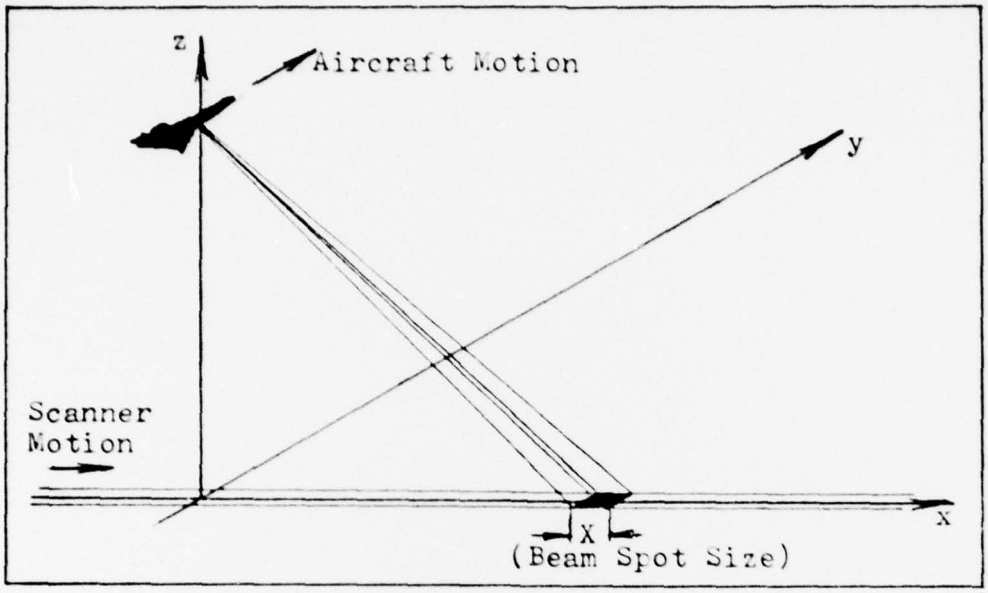

Fig. 1. Raster Scanner Geometry

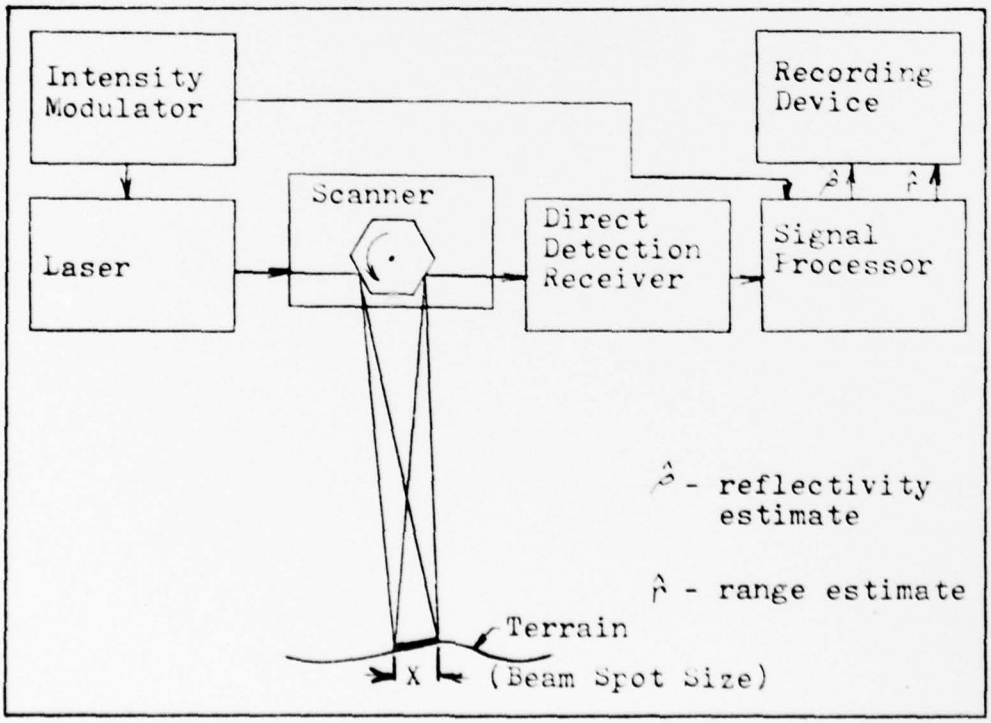

Fig. 2. Laser Line Scanning Sensor Block Diagram

Mod 2π ambiguities. Thus, the range measured is relative range and will contain a $c/2f_m$ range ambiguity, where c is the velocity of light and f_m is the frequency of the detected harmonic.

Problem

The purpose of this thesis is to analyze the spatial filtering effects of the finite beam size, and to determine the interaction between the various laser scanning sensor parameters and the terrain characteristics. This analysis of the spatial filtering can be used to determine the sensor's fundamental limits of resolution. The primary goal of this thesis is to examine the image degradation caused by the spatial filtering. In addition, there is an interest in extending the analysis of the spatial filtering to the analysis of the spatial filtering for the design of a forward looking sensor utilizing small grazing angles. Previous work done by Robinson (Ref 2) included an analysis of the sensor with sinusoidal scanner modulation which determined the conditions for no distortion of the terrain input signals by the spatial filtering. These results form the main approach to the problem and will be reviewed in the next chapter. Also, research has been conducted on several promising types of temporal modulation for the laser (Ref 3), but the analysis needs to incorporate the effects of spatial filtering to be complete. Such an overall analysis will be used to optimize the sensor performance and will impact future sensor designs.

Assumptions

In order to limit the scope of the problem, several assumptions are made in modeling the spatial filtering for the laser line scanning sensor. First, the receiver is a direct detection receiver. Second, only periodic

temporal intensity modulation or modulation which can be represented as a Fourier Series will be considered. Third, the beam will be modeled as having only one dimension which will be along the scanner direction of motion (x-axis in Figure 1). In turn, the terrain will only be modeled along the same axis. Fourth, the receiver is aligned and functioning properly. Fifth, the receiver noise is wideband noise. Finally, it is assumed that the post detection signal processing will not further distort the desired information.

Thesis Overview

The analysis of the spatial filtering problem starts with a review of the spatial filtering model. A general approach for modeling the terrain as a statistically stationary process is examined. The terrain range and reflectivity are modeled as Gaussian Random Processes. Due to the nonlinear nature of the input range signal, only general relationships between the terrain characteristics and the sensor parameters for no distortion are derived. Because the general problem is beyond the scope of this study, some special cases are examined and analyzed. Specifically, the cases which are analyzed are for constant terrain range and for linearization of the phase modulated range input signal. One other special case which is examined is the case for sampling receivers. This analysis applies to pulse modulation systems.

The following chapter is composed of an analysis for spatial filtering distortion for a single sinusoidal range input along with constant reflectivity. The distortion due to the spatial filtering is modeled as an ideal low pass filter. The range error caused by the distortion from the spatial filtering is added to the range error caused by the distortion from the receiver noise in the phase tracker of

the receiver giving the total range error. The resulting distortion data is plotted in terms of the terrain range characteristics, sensor beam-width, frequency of modulation, and the range error. The distortion results are applied to compute the range error for several specific cases including an extension to the forward looking case.

In the remaining chapter the general results are summarized and some recommendations for solving the general spatial filtering problem for any type of range input are presented.

II. Spatial Filter Model

A one-dimensional spatial filtering model representing the beam filtering process of the terrain range and reflectivity of the laser line scanner was developed by Robinson and Reinman (Ref 2, 4). This model applies only for periodic sinusoidal intensity modulation of the laser, but some crude generalizations can be made for other types of periodic intensity modulation. The model was originally used to determine the conditions under which the terrain range and reflectivity signals would not be distorted. A short review of the model along with the conditions obtained for distortionless received signals are presented in the following sections. This leads to the prime emphasis of this thesis which is to analyze the distortion of the range and reflectivity signals caused by the beam filtering. Because the general case of spatial filtering is not easily analyzed, it is necessary to model and idealize the description of the terrain range and reflectivity, and the beam filtering function.

The received signal at the detector output is represented by the following integral (Ref 2:2):

$$s(t) = P_o \int_{-\infty}^{+\infty} \rho(x)\ b(x-vt)\ f(t - \frac{2r(x)}{c})dx \qquad (1)$$

where $r(x)$ is the slant range from the terrain to the aircraft, $b(x)$ is the beam filtering function, $\rho(x)$ is the terrain reflectivity, v is the scan velocity, $f(t)$ is the temporal intensity modulation, c is the velocity of light, and P_o is the peak optical power which includes the propagation and optics losses. This one dimensional representation of the spatial filtering is valid if the two dimensional beam filtering function, $b(x, y)$, is extremely narrow along the y-axis, or if the range

r(x) is treated as an average of the range values in the y dimension over the beam spot size. Eq (1) is valid for all types of intensity modulation. It is convenient to assume that f(t) is periodic and has the following Fourier Series representation: $\sum_{n=-\infty}^{\infty} c_n e^{+j2\pi n f_m t}$, where f_m is the fundamental frequency and the c_n's are the Fourier Series coefficients. By inserting the Fourier Series representation of f(t) in Eq (1), it can be rewritten as follows:

$$s(t) = P_o \sum_{n=-\infty}^{\infty} c_n \int_{-\infty}^{+\infty} \rho(x)\, b(x-vt)\, e^{+j2\pi n f_m (t-\frac{2r(x)}{c})}\, dx \quad \text{(Ref 2:2)} \quad (2)$$

The Fourier Transform of Eq (2) can be determined using two Fourier Transform theorems, and is the expression in Eq (3),

$$S(f) = P_o \sum_{n=-\infty}^{\infty} \frac{cn}{|v|} B^*(\frac{f-nf_m}{v})\, D(\frac{f-nf_m}{v}) \quad \text{(Ref 2:3)} \quad (3)$$

where B(f) is equal to the Fourier Transform of b(x), and D(f) is equal to the Fourier Transform of $\rho(x)$ exp $(j\frac{4\pi n f_m r(x)}{c})$. For harmonics with nonzero c_n's, the periodic modulation shifts the spectra so that is is centered at multiples of the fundamental frequency. The amount of information received is independent of the scan velocity because both D(f) and B(f) are scaled by v. It is important to realize that the bandwidth of one spectrum alone does scale with v as this will impact the post detector electronics design. Although all the spectral contain range and reflectivity information, the information will vary between harmonics because the range ambiguity interval is different. The constants in front of Eq (3) will be ignored because they do not contribute to the range or reflectivity data. This leads directly to the spatial filter model which Robinson derived (Ref 2) and which is shown in Figure 3. The model in Figure 3 is the equivalent complex model for the detection of any harmonic, nf_m. One important consideration is that the range

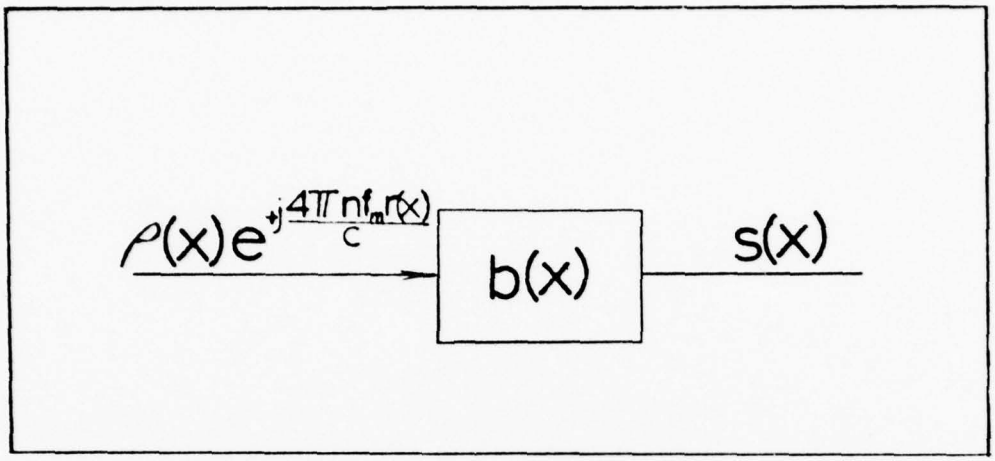

Fig. 3. Spatial Filter Model

data being measured is relative range and may contain Mod 2π ambiguities depending upon λ_m, the fundamental wavelength of the temporal modulation; and the range variations within the beam. Unless otherwise stated, this model will be used throughout the remainder of the thesis. The first approach to the spatial filtering analysis is the stocastic modeling of the terrain parameters.

Gaussian Random Processes Model

An original approach to the spatial filtering problem is to model the terrain range and reflectivity as Gaussian Random Processes (GRP), compute the power spectral density of the input, and determine how the Fourier Spectrum is distorted by the spatial filter. The following assumptions are used to model the terrain as a GRP:

1. $\rho(x)$ and $r(x)$ are statistically independent GRP with zero means.

2. The terrain scene is statistically stationary so that the autocorrelation functions $R_r(x,x')$, the range autocorrelation function, and $R_\rho(x,x')$, the reflectivity autocorrelation function, can be written as

$R_r(d)$ and $R_\rho(d)$ respectively, where $d = x-x'$.

By using the above assumptions and the characteristic function, it can easily be shown that the autocorrelation function of $\rho(x)\exp(+j\frac{4\pi n f_m r(x)}{c})$ is:

$$R_o(d) = R_\rho(d)\exp[-(\frac{4\pi n f_m}{c})^2(R_r(0) - R_r(d))] \tag{4}$$

The Fourier Transform of Eq (4) is the power spectral density and can be written as follows:

$$S_d(f) = e^{-(\frac{4\pi n f_m}{c})^2 R_r(0)} F_d[R_r(d)] * F_d[e^{+(\frac{4\pi n f_m}{c})^2 R_r(d)}] \tag{5}$$

where F_d is the Fourier Transform operator on the variable d. If the bandwidth of the Fourier Transform of $R_\rho(d)$ is B_ρ, and the bandwidth of the Fourier Transform of $\exp((\frac{4\pi n f_m}{c})^2 R_r(d))$ is B_{r_ϕ}, then crudely the bandwidth of $S_d(f)$ is the sum of these two bandwidths. Thus for the input signal to be filtered with no distortion,

$$B_\rho + B_{r_\phi} < B_f \tag{6}$$

where B_f is the spatial bandwidth of the beam filter. Depending upon the characteristics of the range and reflectivity autocorrelation functions, it is usually very difficult to compute B_ρ and B_{r_ϕ}. Another bandwidth measure is mean squared bandwidth of the power spectral density (Ref 5:100). It can be used to rewrite Eq (6) as follows:

$$\sqrt{\overline{B_\rho^2}} + \sqrt{\overline{B_{r_\phi}^2}} < \sqrt{\overline{B_f^2}} \tag{7}$$

where $\overline{B_\rho^2}$ is the reflectivity mean squared bandwidth, $\overline{B_{r_\phi}^2}$ is the mean squared bandwidth of the Fourier Transform of $\exp((\frac{4\pi n f_m}{c})^2 R_r(d))$, and $\overline{B_f^2}$ is the mean squared bandwidth of the filter. Eq (7) can be rewritten in terms of the beam spot size, the mean-squared bandwidth of the range

process, $\overline{B_r^2}$, using some previously derived results (Ref 2:5-6):

$$\sqrt{\overline{B_\rho^2}} + \sqrt{\frac{1}{4}\left(\frac{4\pi n f_m}{c}\right) R_r(o)\,\overline{B_r^2}} < \frac{1}{X^2} \qquad (8)$$

In Eq (8) $R_r(0)$ is the mean squared range variation, and $1/X^2$ (X is the beam spot size) is approximately equal to the mean squared bandwidth of the spatial filter. $\overline{B_{r_\phi}^2}$ is generally much larger than $\overline{B_r^2}$. For no distortion and the input bandwidth $\overline{B_\rho^2}$ being small, $\overline{B_r^2}$ can be proportionally large compared to the case for $\overline{B_\rho^2}$ being large. Similarly, if the input bandwidth $\overline{B_r^2}$ is small, $\overline{B_\rho^2}$ can be large compared to the case for $\overline{B_r^2}$ being large. Thus, there is an interaction between r(x) and ρ(x) which depends on the respective input bandwidths and directly affects the distortion of the resulting output signals.

Distortion Effects

The GRP model is good for determining the conditions for no distortion, but it is substantially troublesome to use for determining how the signal will be distorted if the terrain input signal, $\rho(x)\exp(\frac{4\pi n f_m r(x)}{c})$, has a bandwidth which exceeds the bandwidth of the spatial filter. Typically, this condition is encountered for rough terrain that has sharp edges, and rapidly varying terrain heights and changes in reflectivity, and will result in some distortion of the terrain range and reflectivity signals. The distortion process caused by the beam filtering is a linear process; however, the phase modulated range input signal is nonlinear, thus the resultant output signals which are filtered will be nonlinear. This problem is the standard amplitude-phase modulated signal which is filtered; and is studied by Middleton (Ref 6:628-632), and many others in the communications field. Unfortunately, this problem does not yield

any exact, tractable analytic solutions, thus most solutions are generally arrived at by numerical means. However, there are some specialized results which are made possible by modeling the terrain range variation, the terrain reflectivity, and the beam function for idealized cases.

Linear Approach

One approximation which considerably simplifies the spatial filtering problem is the series expansion of the exponential and truncation of this series to include just the first two terms. Now, the terrain range input to the filter is linear in r(x) and the spatial filtering is equivalent to the low pass filtering of the product of two amplitude modulation processes. The linear model representation of the beam spatial filtering is shown in Figure 4. For the linear approxima-

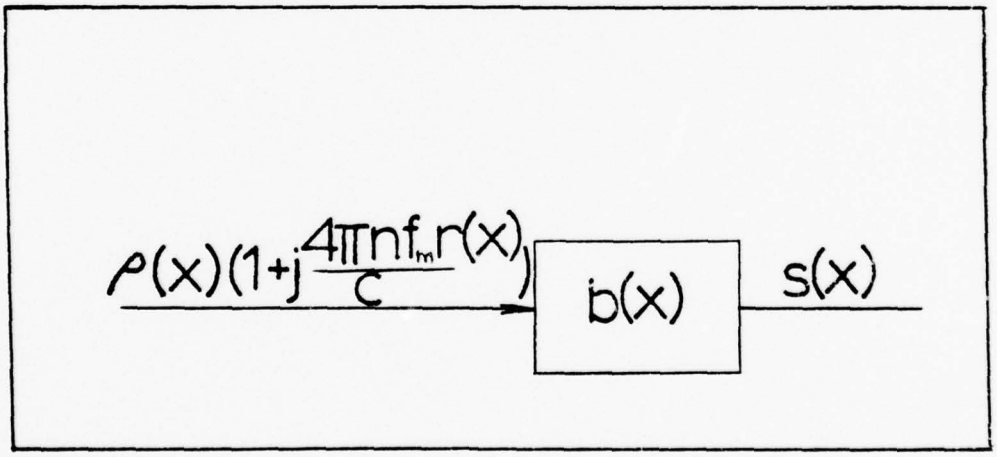

Fig. 4. Linear Approximation for Spatial Filtering

tion to be valid, the following inequality must hold, $\frac{4\pi n f_m r(x)}{c} << 1$. Typically, this means that the left side of the inequality must be less than $\pi/12$, or the phase variations are less than 15°. The linear case ensures that the bandwidth of the phase modulated process is narrowband. If the variations in range are small, then for no distortion the spatial frequency variations of the range can be considerably larger than when

compared to the general phase modulation case. When the n=0 term is detected, there is a reflectivity term without any dependence on r(x). If this reflectivity term could be detected, it could be used to remove the reflectivity dependence of the other terms, and if done properly could decrease the spatial bandwidth on the input signal to the spatial filter. (This discussion on the removal of the reflectivity dependence is applicable to the general problem, not just the linear approximation.)

Constant Range

Another method for analyzing the beam interaction with the terrain reflectivity is to assume that the terrain range is constant, so that Eq (1) can be written as:

$$s(t) = \int_{-\infty}^{+\infty} b(x-vt)\ f(t-c_1)\ \rho(x)dx \qquad (9)$$

where c_1 is a constant range term. The Fourier Transform of Eq (9) is the convolution expression in Eq (10), where F(f) is the Fourier Transform

$$S(f) = e^{-jc_1}F(f) * \frac{1}{|v|} B^*(f/v)R(f/v) \qquad (10)$$

of f(t), B(f) is the Fourier Transform of b(x), and R(f) is the Fourier Transform of $\rho(x)$. The whole process can be modeled in the time domain as shown in Figure 5. Therefore, for the constant range assumption, only

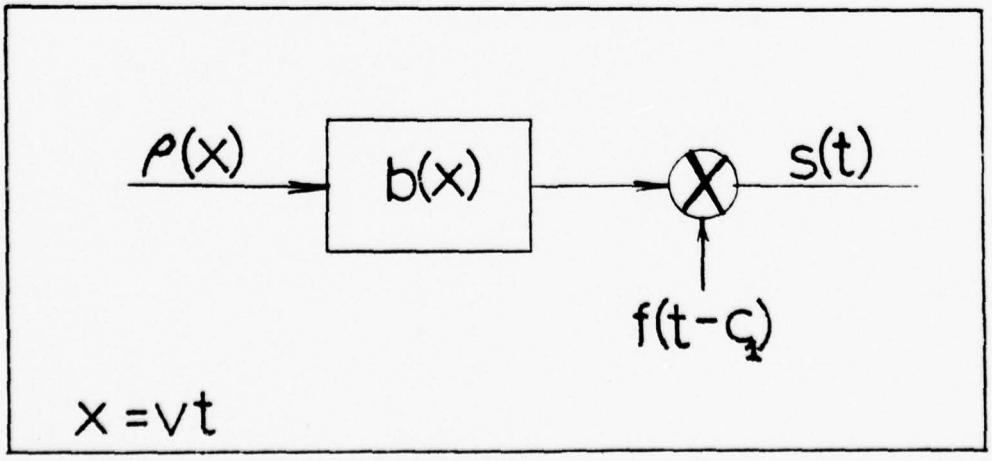

Fig. 5. Constant Range Spatial Filter Model

the reflectivity variation will be observed. Also, the distortion which will be observed is simply the low pass filtering of an amplitude modulated signal. This implies that the sensor will be able to resolve reflectivity variations along the x-axis down to the size of the beam spot size. The entire constant range discussion is analogous to observing the Fourier Series component for n=0 as previously discussed under the linear approximation.

Another Representation-Sampling

The effects of spatial filtering on the terrain signals can be characterized for sampling receivers. This is particularly valuable because the sampling concepts can be used to extend the spatial filtering results from the case of sinusoid modulation to pulse types of periodic modulation to pulse types of periodic *modulation for the scanner*. Initally, the terrain range will be assumed to be constant, so that only the variations in reflectivity will be observed. Using the constant range representation which was previously presented, the beam spatial filtering can be represented as shown in Figure 6, where $\rho'(x)$ is the filtered reflectivity. For a pulse modulated system, $\rho'(x)$ would be

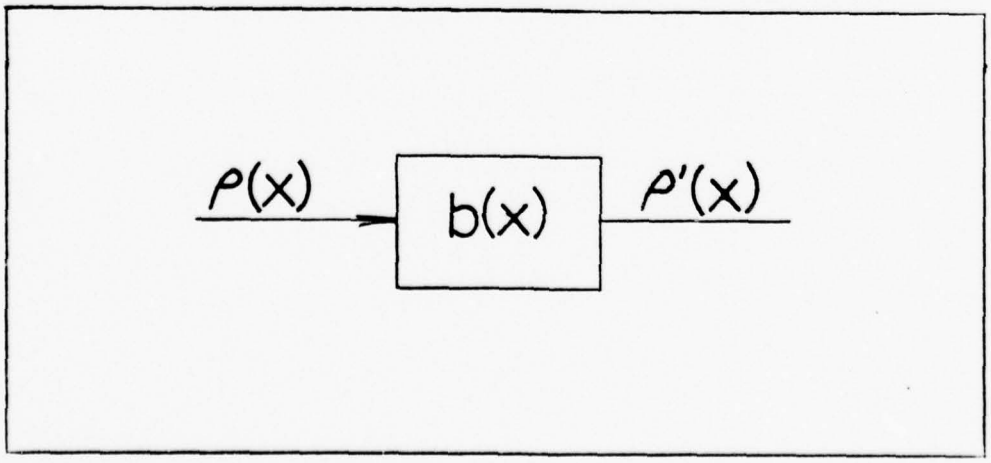

Fig. 6. Reflectivity Spatial Filtering for Constant Range

sampled at the pulse repetition rate, and the sampled $\rho'(x)$ would be used to reconstruct $\rho'(x)$. To reconstruct $\rho'(x)$, it is necessary to determine how close $\rho'(x)$ should be sampled along x, or what the pulse repetition rate should be. Since $\rho'(x)$ is bandlimited by $b(x)$ which has an approximate bandwidth of $1/X$, then $\rho'(x)$ should be sampled at $2/X$ or twice every beamwidth to prevent aliasing. If this type of argument is expanded to include the terrain range input, the detected signal will also be bandlimited by the spatial filter to $1/X$.

This representation can be extended to look at the more general problem which encompasses other types of periodic modulation for the scanner. This problem can be examined by taking the inverse Fourier Transform of Eq (3), which can be represented by a sum of signals which are demodulated to baseband and passed through sampling filters and is given by Eq (11). In principle, Eq (11) could be applied

$$s(x) = \sum_{n=-\infty}^{\infty} c_n \rho(x) e^{+j\frac{4\pi r(x) n f_m}{c}} * b(x) \qquad (11)$$

to determine the output signal by using an infinite number of receivers, where each receiver detects a different spatially filtered harmonic.

From this modeling of the sampling receiver two conclusions can be drawn. First, for a constant range sampling receiver, the reflectivity variations which are on the order of the spot size will be resolved providing that the spatial filter output is sampled at $2/X$. Similarly, for the sampling receiver which simultaneously detects reflectivity and range variations, the minimum detectable range or reflectivity variations along the x-axis will be several beamwidths depending upon the bandwidth of the input signal to the spatial filter. Clearly, the distortion of the input terrain signal is a function of its bandwidth.

Second, no matter what pulse repetition rate is chosen, assuming that aliasing is not occurring, the maximum bandwidth of the detected signal is the spatial filter bandwidth.

III. Distortion Analysis and Results

Within this chapter, the distortion which results from the spatial filtering is discussed and analyzed. As previously mentioned, the distortion is caused by the bandlimiting of the spatial filter. The distortion process is of considerable importance in analyzing the laser line scanning sensor because the resolution of the sensor is limited by the distortion process. Unless a measure of distortion is defined, the term distortion is rather nebulous. For the purpose of this thesis, distortion is defined in terms of the mean squared error of the detected signals. For other measures of distortion and their calculation, the appropriate communication literature can be consulted (Ref 7-15). After a measure of distortion is chosen, somehow the distortion must be computed. Unfortunately, the modulation process is a nonlinear process, and thus the distortion can only be computed by numerical analysis with the aid of a digital computer. Once the distortion has been modeled, it is desirable to compute the distortion in terms of the sensor and the terrain parameters. After this step is accomplished, the distortion data can be used to optimize the sensor parameters for minimum distortion, given a particular set of terrain parameters.

General Analysis of the Spatial Filtering Distortion

To make a general analysis of the spatial filtering distortion, it is desirable to express the distortion in terms of an input-output relation. Although this representation simplified the problem, it does not provide an analytical solution for modeling the distortion effects. Figure 7 is the illustration of the spatial filter representation for the distortion input-output relation. Each output signal, $\rho'(x)$ and

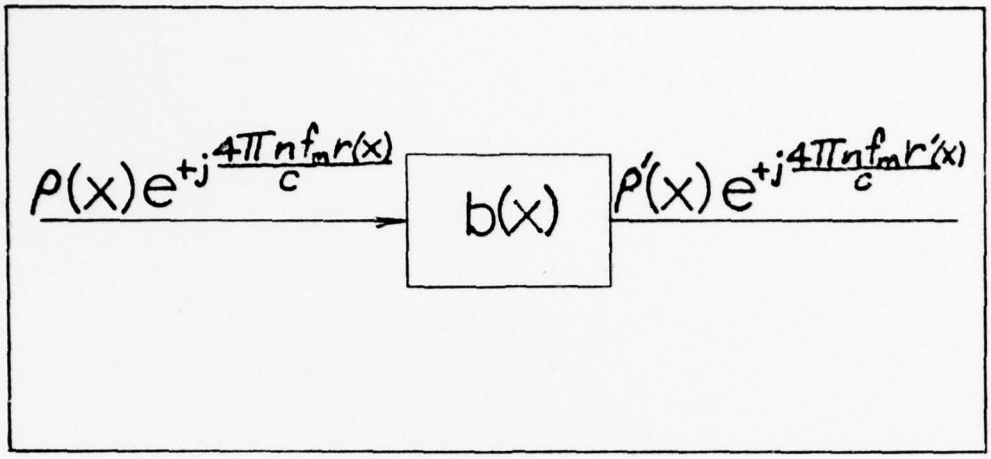

Fig. 7. Spatial Filtering with Output Signals in Terms of the Detected Terrain Signals

r'(x), is dependent upon both input terrain signals, ρ(x) and r(x). Furthermore, ρ'(x) and r'(x) can be exactly represented in terms of the slant range, the reflectivity, and the beam intensity function as illustrated in Eq (12) using the trigonometric representation of a complex

$$\rho'(x) = \sqrt{(\rho(x)\cos(\frac{4\pi n f_m}{c} r(x))*b(x))^2 + (\rho(x)\sin(\frac{4\pi n f_m}{c} r(x))*b(x))^2} \quad (12a)$$

$$r'(x) = \frac{c}{4\pi n f_m} \tan^{-1}\left(\frac{(\rho(x)\sin(4\pi n f_m \frac{r(x)}{c}))*b(x))}{(\rho(x)\cos(4\pi n f_m \frac{r(x)}{c}))*b(x))}\right) \quad (12b)$$

exponential function, where the asterisk represents the operation of convolution. Implementation of Eq (12) is possible, but it would require two convolutions for each signal; the results would only apply to a specific case, and the terrain parameters would have to be modeled in great detail. One way to solve this general problem is to use Fast Fourier Transform techniques, and implement the problem on a digital computer, but this is beyond the scope of this effort.

Specialized Distortion Analysis

The general problem can be solved, but the solution requires an extensive numerical analysis, and the solutions are very specialized. Therefore, some simplifications and idealizations are necessary to make the problem more tractable and to provide some useful results. Probably, the simplest idealization is to assume that the linear approximation is valid. The outgrowth of this condition is that the phase modulated range signal is narrowband and this portion of the signal behaves as an amplitude modulated signal. Thereby, the linear case is analogous to having an input signal which is the product of two amplitude modulated signals. The advantage of the linear case is that the distortion process for amplitude modulation is analytically tractable and well understood. The linear case can be implemented for the sensor by sufficiently decreasing the fundamental frequency of modulation until the phase variation is less than 15°. Unfortunately, when the fundamental frequency is decreased, the accuracy of the relative range decreases also. Another consequence of the linear approximation which also applies to the general problem is that at the center frequency of the output, where $n=0$, the reflectivity term is decoupled from the range term. This reflectivity term could be separately detected and used to separate the reflectivity dependence from the input or output of the spatial filter.

Two methods are presented for removing the reflectance dependence. One method decouples the reflectivity at the input, while the second scheme decouples the reflectivity term at the output.

1. Decoupling the reflectivity term at the input to the spatial filter can be implemented by using a two beam scanner where the first beam illuminates the terrain with a cw signal and is used to recover the

reflectivity signal. The reciprocal of the reflectivity signal is used to amplitude modulate the second beam which follows directly behind the first beam. Thus, the reflectivity dependence is nearly removed and only the phase modulated range signal is filtered. This method is expensive to implement because of the additional equipment required, but the output signal is completely decoupled from the reflectivity.

2. Decoupling the reflectivity at the output can be accomplished by using a d.c. receiver pickoff and dividing the dependency of this signal out of the existing signal. However, there is one serious consideration, the distortion terms will still be present even though the reflectivity dependence has been removed. These distortion terms could cause errors in the detected terrain range signal.

There are two other specialized cases which are considerably simpler to analyze, constant range and constant reflectivity. The constant range case is of little practical consequence; but it does illustrate a particular case, namely, the lowpass filtering of an amplitude modulated signal where the distortion process is well understood. In the case of constant reflectivity, it is now reasonable to accomplish a numerical analysis of the distortion because the input terrain signal is strictly a phase modulated signal, and the resulting analysis is much easier. Using this assumption of constant reflectivity, the range distortion will be modeled and computed.

Range Distortion Modeling

The distortion of the range signal can be easily modeled, and numerical results can be obtained by assuming that the reflectivity is constant and that the terrain range can be modeled as a periodic function. The modeling of the terrain reflectivity as a constant is valid for

slowly varying reflectivity or when the reflectivity dependence is removed as previously illustrated. The periodic function representation of r(x) is an appropriate comparison to the real terrain over short distances along the x-axis which could include up to several beamwidths. Actual calculations of the distortion to the range signal will include additional assumptions in order to simplify the numerical analysis.

Fourier Series Representation of the Phase Modulated Periodic Range Function

A periodic function which is phase modulated can be represented as a product of Bessel Fourier Series. The terrain range which is assumed to be a periodic function has a Fourier Series representation, $\sum_{\ell=-\infty}^{\infty} a_\ell e^{+j2\pi f_K \ell x}$, where the a_ℓ's are the complex Fourier coefficients, and f_k is the fundamental spatial frequency of the range function. The phase modulated range function can be expressed as follows using the trigonometric representation of a complex exponential:

$$e^{+j\frac{4\pi n f_m}{c} r(x)} = e^{+j\frac{4\pi n f_m}{c} \sum_{\ell=-\infty}^{\infty} a_\ell \exp[+j2\, f_K \ell x]} \tag{13a}$$

$$e^{+j\frac{4\pi n f_m}{c} r(x)} = \prod_{\ell=-\infty}^{\infty} \exp[+j\frac{4\pi n f_m}{c}\, a_\ell(\cos 2\pi f_K \ell x + j\sin 2\pi f_K \ell x)] \tag{13b}$$

Using the Bessel function identities of a complex exponential with a sine or cosine argument, the right side of Eq (13b) can be rewritten as an infinite product of Bessel Series as shown in Eq (14), where a_ℓ equals $|a_\ell| e^{+j\theta_\ell}$.

$$e^{+j\frac{4\pi n f_m}{c} r(x)} = \prod_{\ell=-\infty}^{\infty} \sum_{q=-\infty}^{\infty} (1 + j^q) J_q(\frac{4\pi n f_m}{c} |a_\ell|) e^{+j^{q(2\pi f_K \ell x + \theta_\ell)}} \tag{14}$$

For example, if the range is a single sinusoid, where $r(x) = r_m \sin(2\pi f_r x)$, then its Bessel Fourier Series representation is:

$$e^{+j\frac{4\pi n f_m r_m \sin(2\pi f_r x)}{c}} = \sum_{q=-\infty}^{\infty} J_q\left(\frac{4\pi n f_m r_m}{c}\right) e^{+j 2\pi f_r x q} \qquad (15)$$

If $\left(\frac{4\pi n f_m r_m}{c}\right)$ is replaced by β (which is usually interpreted as the modulation index), Eq (15) can be rewritten as a real, plus an imaginary infinite series of the following form:

$$e^{+j\beta \sin 2\pi f_r x} = J_o(\beta) + 2[J_2(\beta)\cos 2\pi(2f_r)x + J_4(\beta)\cos 2\pi(4f_r)x + \ldots]$$
$$+ 2j[J_1(\beta)\sin 2\pi f_r x + J_3(\beta)\sin 2\pi(3f_r)x + \ldots] \qquad (16)$$

This form of the phase modulated range signal can be easily used to evaluate, by means of numerical analysis, the spatial filtering distortion.

Sensor Distortion Modeling for a Sinusoid Range Input

For ease of computation, the terrain range signal is assumed to be a single frequency periodic sinusoid of the form $r(x) = r_m \sin(2\pi f_r x)$, where r_m is the peak amplitude range variation and f_r is the spatial frequency of the terrain range input. Two sources of distortion are considered in the modeling of the range error for the laser line scanning sensor. Besides distortion being caused by the spatial filtering, there will be some range error induced by the receiver noise within the Phase Locked Loop (PLL) circuit which is used to track the phase of the detected signal. The two distortion processes are independent and each interacts with the range signal as illustrated in Figure 8. The detector noise is assumed to be wideband in order to model the phase variance of the PLL output, and is modeled as shown in Figure 9. The important result from Figure 9 is that the phase variance is equal to 1/SNR, where SNR is the SNR in the closed loop of the PLL, B_L (Ref 3:15). (This is not to be confused with the bandwidth of the spatial filter.) The phase variance

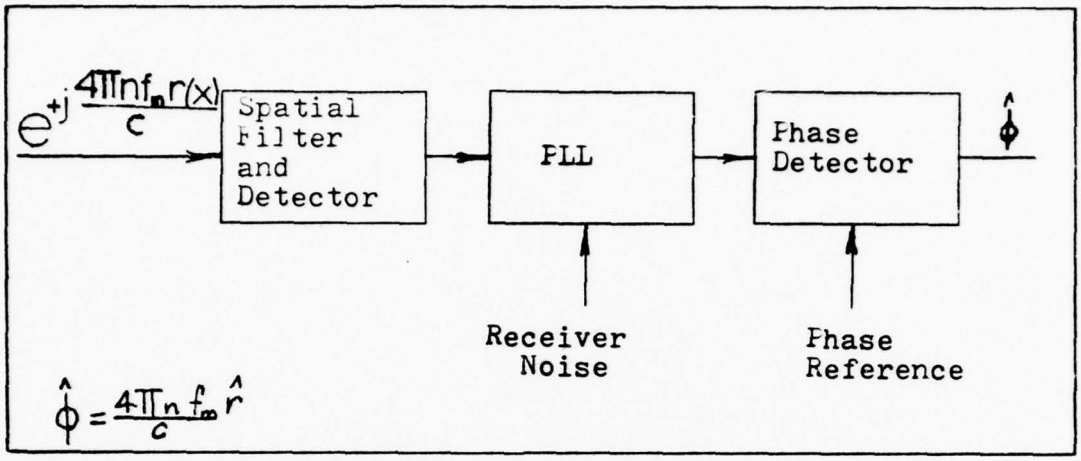

Fig. 8. Range Distortion Processes for the Laser Line Scanning Sensor

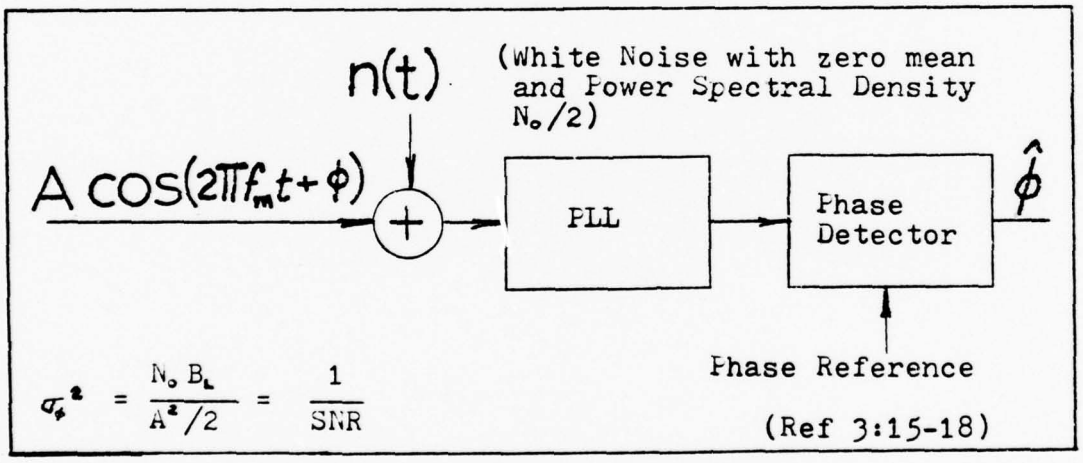

Fig. 9. Phase Variance in the PLL

can be directly related to the range variance by using the relation, $\phi = \frac{4\pi n f_m r}{c}$. Thus, the range variance can be expressed as follows:

$$\sigma_r^2 = \left(\frac{c}{4\pi n f_m}\right)^2 \left(\frac{1}{SNR}\right) \qquad \text{(Ref 3:15-16) (17)}$$

For the model of the phase variance of the PLL in the receiver, it is assumed that the PLL is operating in its linear region which implies that the phase variance must be below a certain threshold. Typically, this threshold is chosen to be .25 (Ref 3:16-17), or that the closed

loop SNR of the detected signal must be greater than four. From the model of the range error caused by the receiver noise in the PLL, it is apparent from the reciprocal relation in Figure 9 that as the SNR increases, the range error decreases. From Eq (17), it is apparent that as the modulation frequency of the laser is increased, the range error decreases.

Using the constant reflectivity assumption and setting r(x) equal to a sinusoid, the spatial filter model can be represented as in Figure 10. If the Bessel Series representation of Eq (15) is used and b(x) is

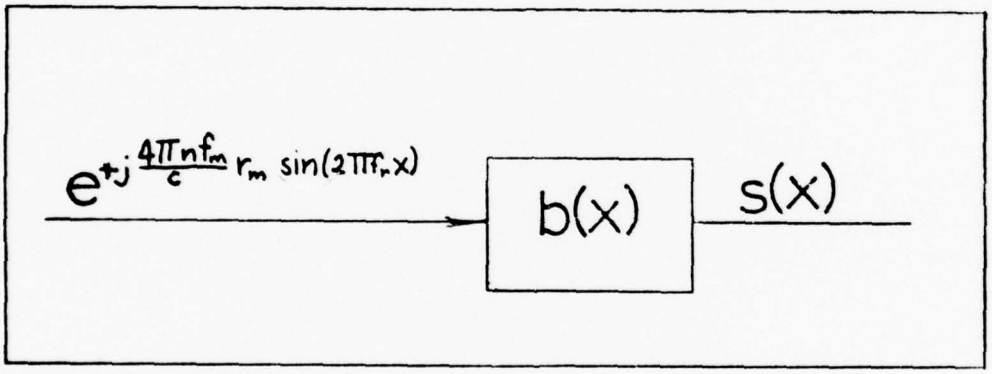

Fig. 10. Single Sinusoid Range Input

approximated as an ideal low pass filter, then the output can be easily represented in terms of the Bessel Series input as shown in Figure 11, where N equals the largest integer portion of the bandwidth of the spatial filter divided by the frequency of the sinusoidal range variation. The approximation of b(x) as an ideal low pass filter is a reasonable simplification since the beam intensity function is typically Gaussian shaped which is comparable to the $\frac{\sin 2\pi fx}{\pi f}$ function up to its first zero The output of the spatial filter is a finite Bessel Series which is easily separated into real and imaginary parts by using the Bessel Series representation of Eq (16). The output phase can be expressed in

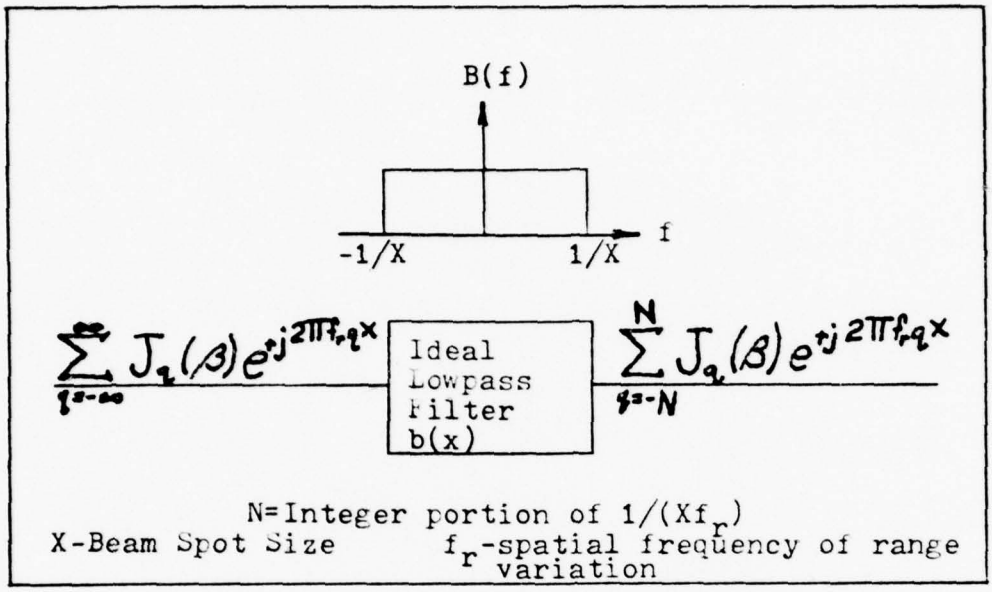

Fig. 11. Output Representation of the Spatial Filter

the following form:

$$\phi = \tan^{-1}\left(\frac{\text{imaginary terms of Bessel Series [Eq (16)]}}{\text{real terms of Bessel Series [Eq (16)]}}\right) \qquad (18)$$

This expression for the output phase of the spatial filter is used to compute the phase error by subtracting the output phase from the input phase; however, the phase error changes according to the value of x. A measure of the phase distortion which accounts for these changes is the integrated mean squared phase error which is the phase error squared and averaged over the period of the sinusoid range input, zero to 2π. Eq (19) is the expression for the integrated mean squared phase error. The computed phase errors are limited to Mod 2π to correspond to the relative phase measurement by the sensor. The mean squared range error is computed

$$\overline{\psi^2} = \frac{1}{T}\int_0^T (\phi(x) - \theta(x))^2 dx \qquad (19)$$

by dividing the mean squared phase error, $\overline{\psi^2}$, by $(\frac{4\pi n f_m}{c})^2$. If ψ^2 is divided

by β^2, then the result is $\frac{\overline{r_e^2}}{r_m^2} = \frac{\overline{\psi^2}}{\beta^2}$ ($\beta = \frac{4\pi n f_m r_m}{c}$), where $\overline{r_e^2}$ is the mean squared range error. This is a convenient form for analyzing the distortion because it incorporates the maximum amplitude variations of the range. From this discussion of spatial filtering, it should be noted that as the frequency of modulation increases, so does the range distortion error because the phase error increases when the argument of the Bessel Functions in Eq (18) increase.

The total mean squared error is computed by adding the distortion from the PLL and the spatial filtering. For low frequencies of modulation, the total distortion error is dominated by the receiver noise distortion process, while at high frequencies of modulation the total distortion is dominated by the spatial filter distortion process. Somewhere in between, there is a frequency of modulation where the range distortion is minimal, i.e., optimum modulation frequency.

One other point which needs to be addressed is that the SNR depends on the bandwidth of the PLL. For comparative distortion calculations, it is assumed that the closed loop bandwidth of the PLL equals the bandwidth of the spatial filter. Thereby, the spatial filter bandwidth varies according to the beam spot size, and it is necessary to normalize the PLL range variance which is given in Eq (17) by multiplying it by N ($N = 1/(Xf_r)$), where different N's relate to different beam spot sizes. This normalized SNR will be designated by SNR_{norm}.

Distortion Computations and Results

Distortion results were evaluated by using the sinusoidal range model. Actual calculations were computed on a CYBER 74 computer, and the Bessel Functions were calculated by an IBM 360 subroutine called

BESJ. A brief list of the assumptions used for making the distortion computations are as follows:

1. The temporal scanner modulation is periodic and only a single harmonic is processed by the receiver.
2. The terrain reflectivity is constant over several beamwidths or its dependency has been removed from the input signal of the spatial filter.
3. The terrain range variation is modeled as a single sinusoid.
4. The beam function, b(x), is modeled as an ideal low pass filter.
5. The detector noise is wideband.
6. The PLL is operating in the linear region.
7. The loop bandwidth of the PLL is equal to the spatial filter bandwidth.

The numberical integration of Eq (19) is implemented by using 2000 intervals of integration. For convenience, the distortion data is presented as plots of $\frac{\overline{r_e^2}}{r_m^2}$ versus β (the phase modulation index), where β is equal to $(\frac{4\pi n f_m r_m}{c})$. In all cases considered, only the first harmonic of the periodic signal is processed by the receiver (i.e., n = 1); and henceforth, n will be dropped from the expressions of β. Figures 12-18 are the plots of $\frac{\overline{r_e^2}}{r_m^2}$ versus β for comparisons of different beam spot sizes (N as related to f_r and X) and for various SNR_{norm}'s and will be discussed later. The absolute SNR is related to the normalized SNR by the following expression:

$$SNR_{abs} = SNR_{norm} - 10 \log N \qquad (20)$$

where SNR_{abs} is the absolute SNR. The plots of the range distortion data can be applied to distortion calculations when the loop bandwidth of the

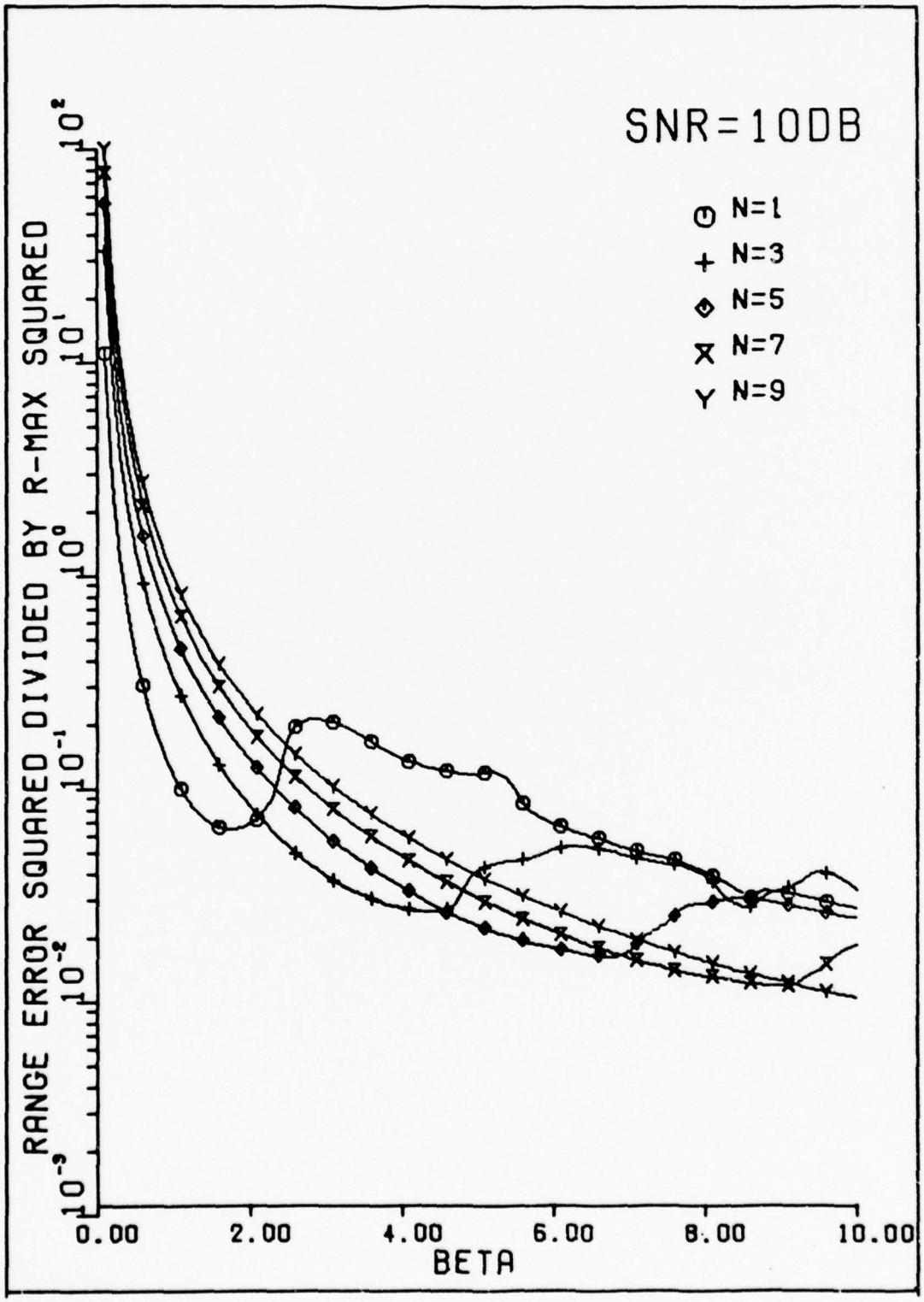

Fig. 12. Normalized Mean Squared Range Error Versus Beta for SNR = 10db

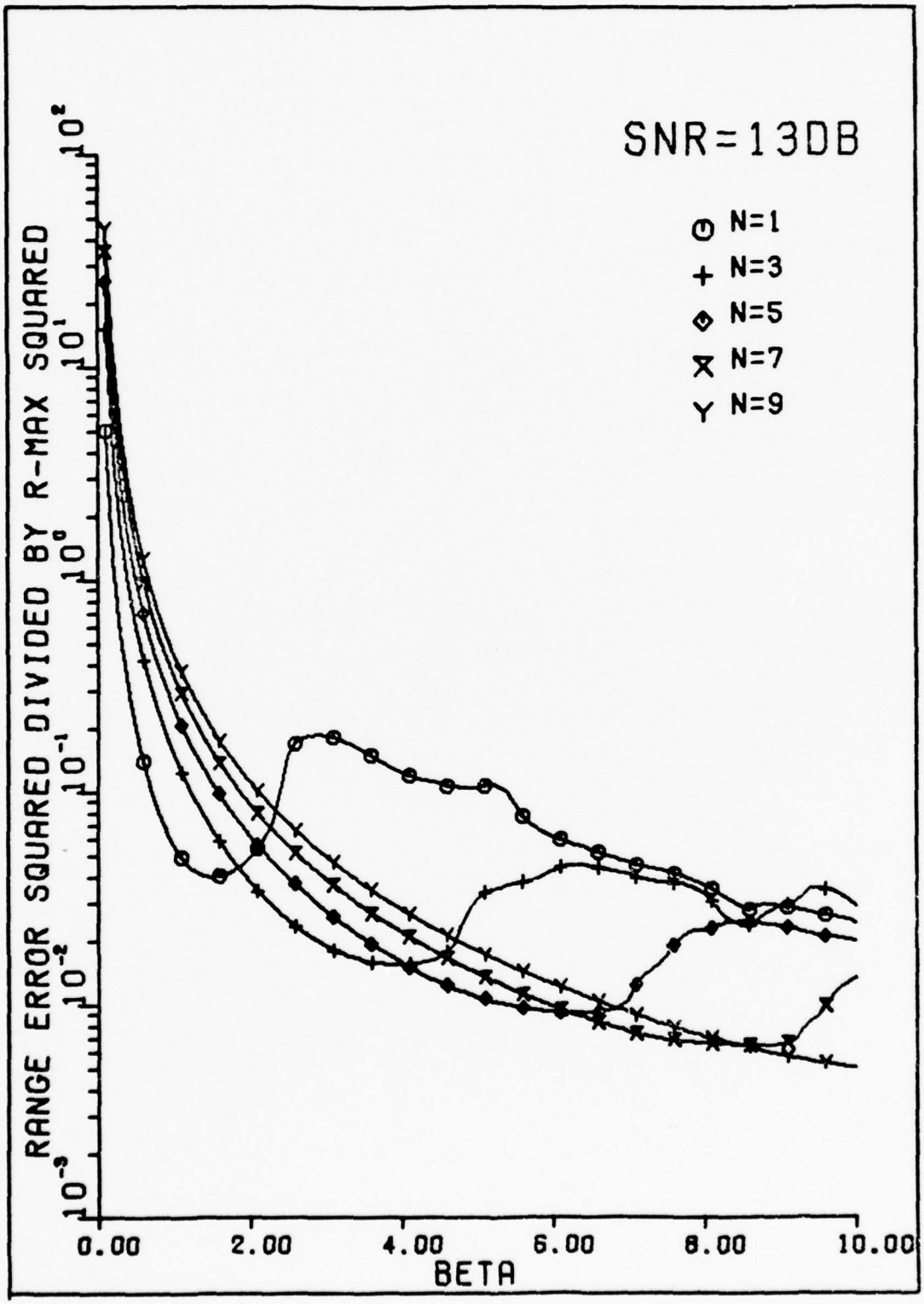

Fig. 13. Normalized Mean Squared Range Error Versus Beta for SNR = 13db

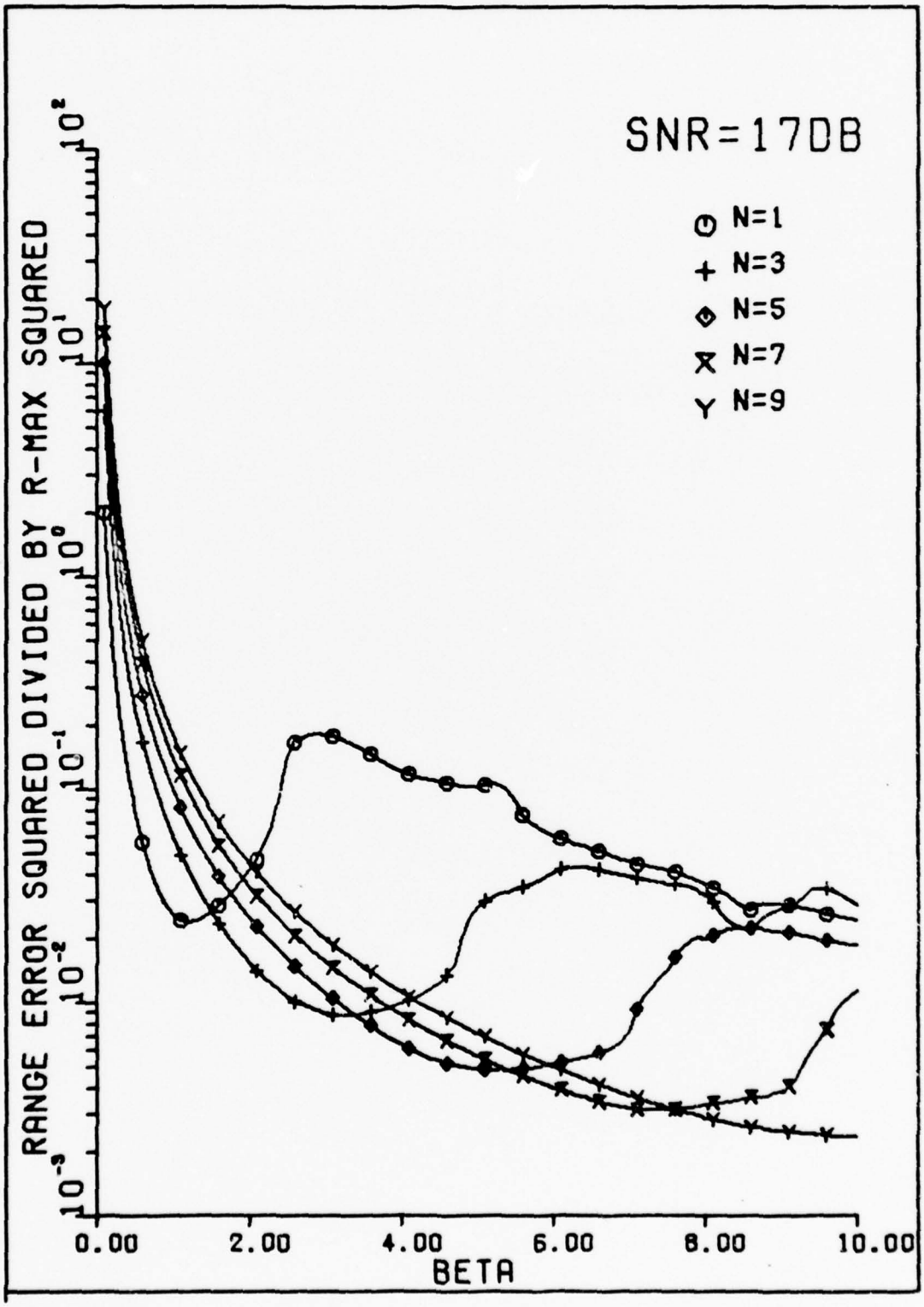

Fig. 14. Normalized Mean Squared Range Error Versus Beta for SNR = 17 db

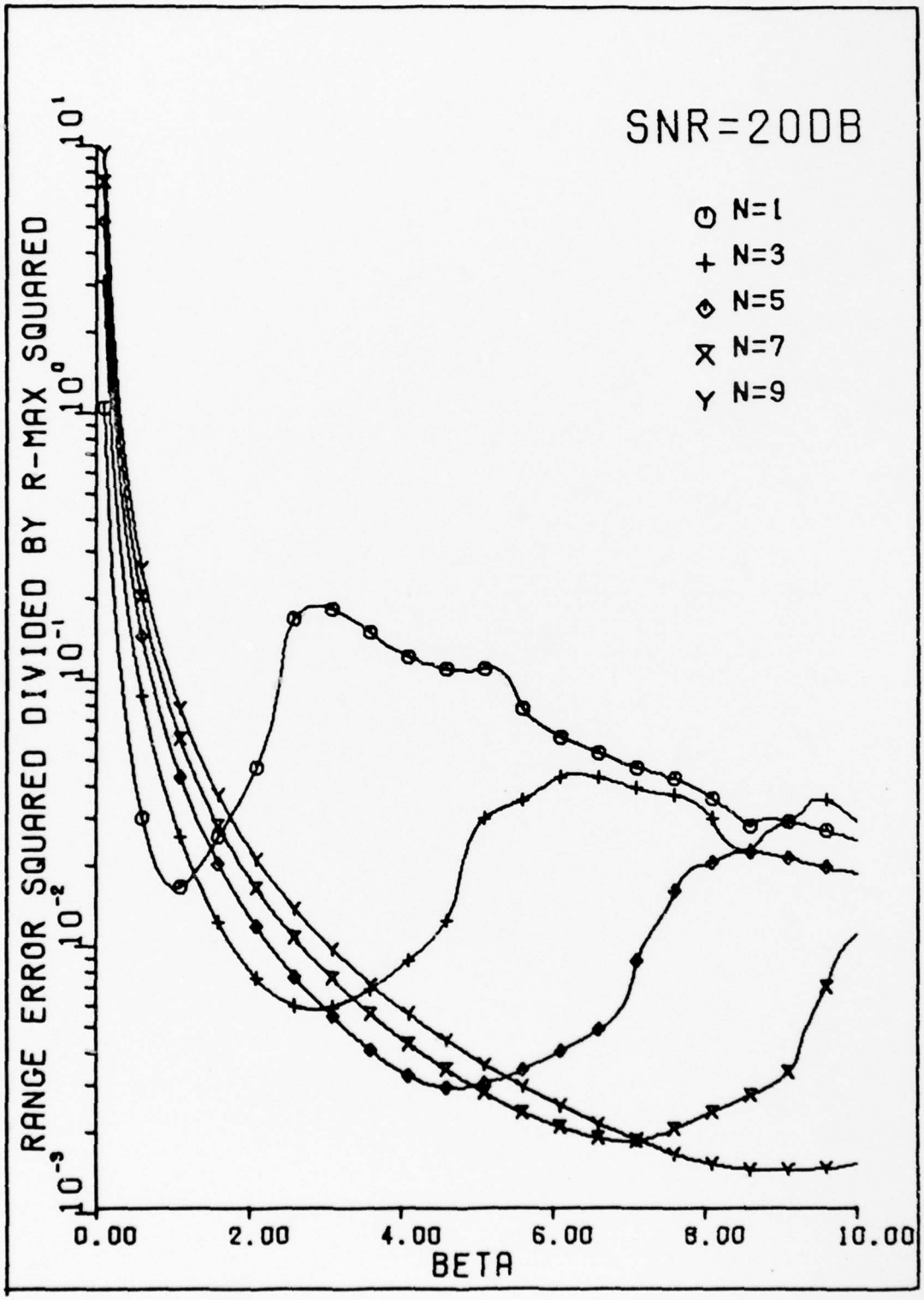

Fig. 15. Normalized Mean Squared Range Error Versus Beta for SNR = 20db

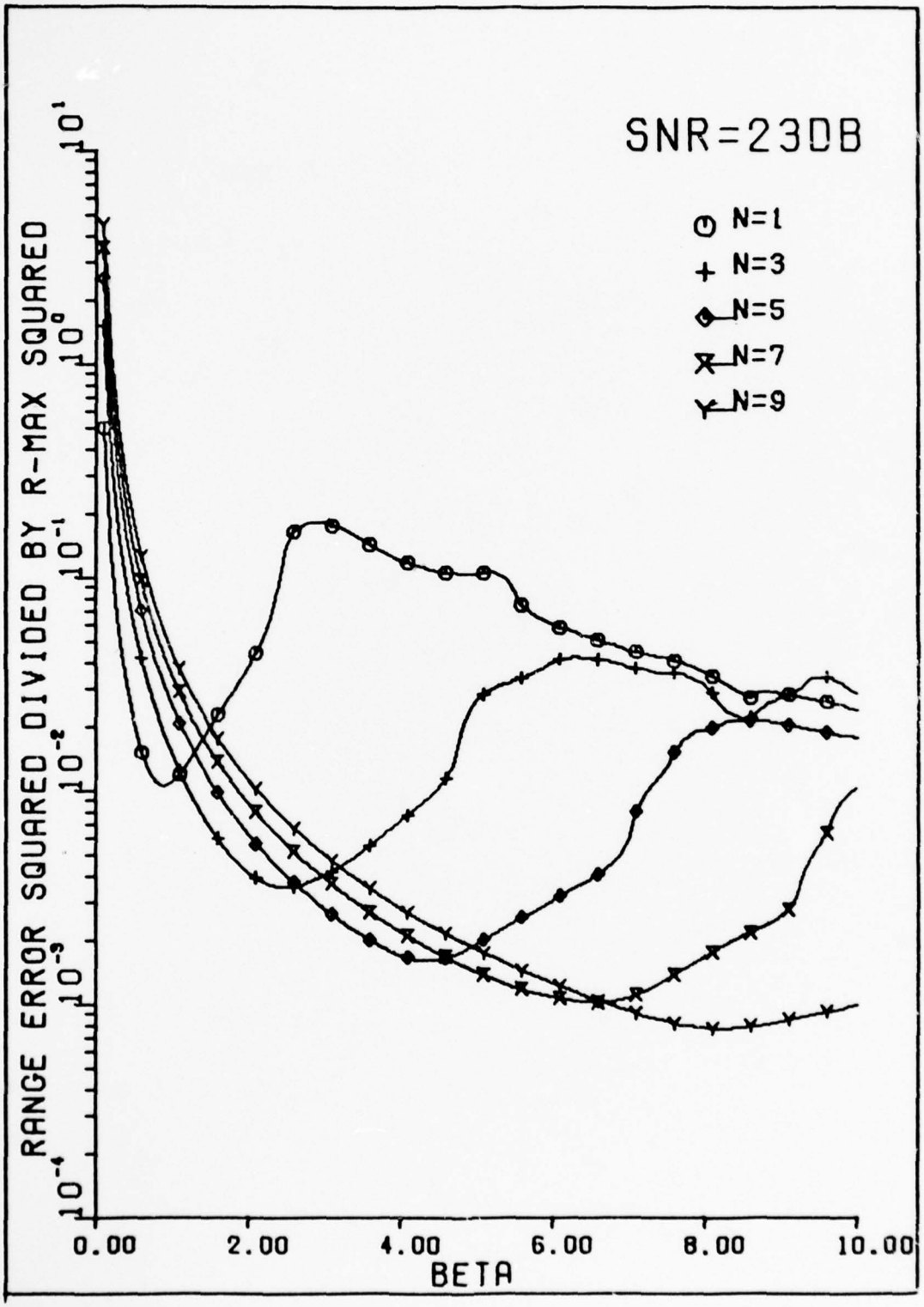

Fig. 16. Normalized Mean Squared Range Error Versus Beta for SNR = 23db

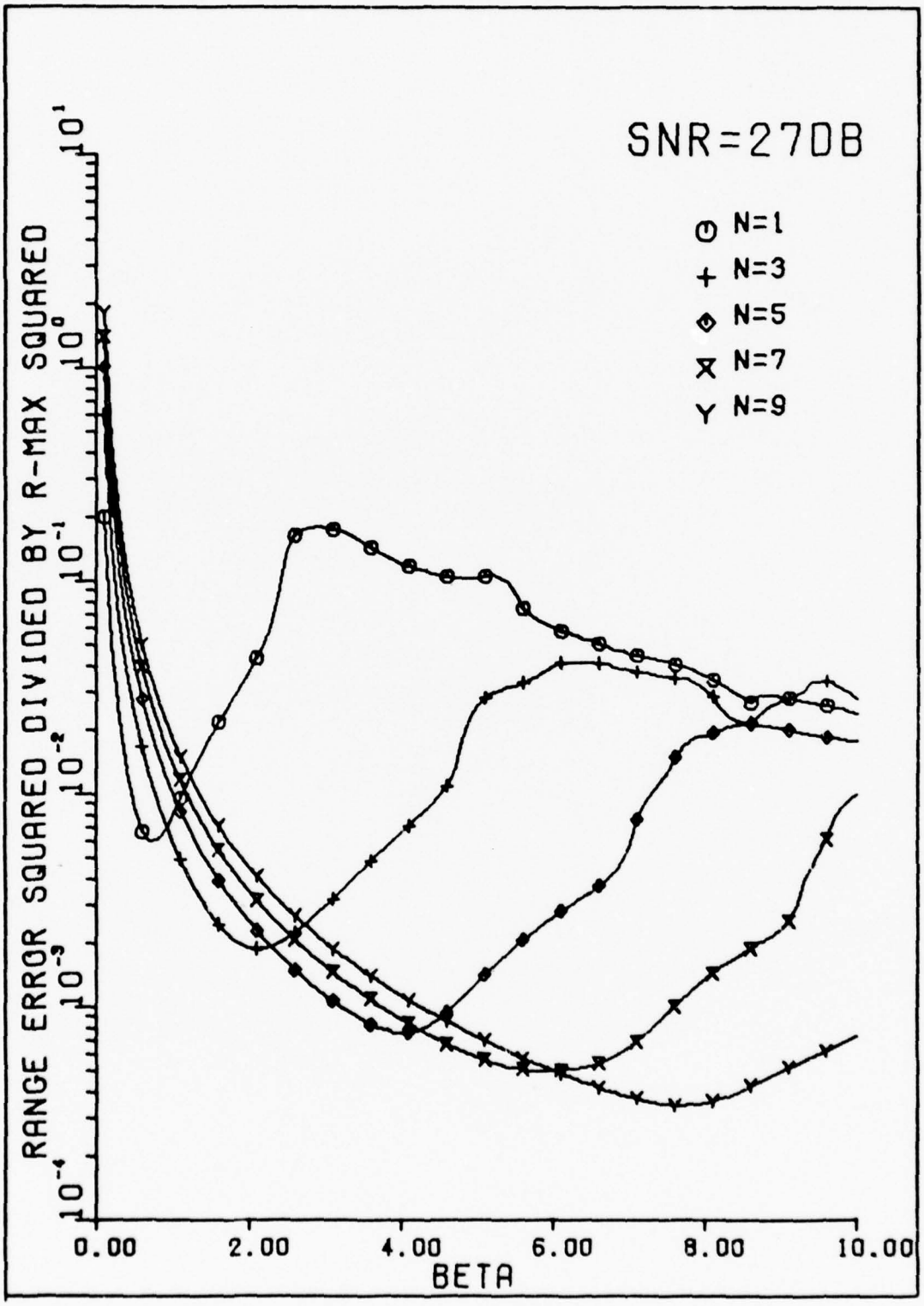

Fig. 17. Normalized Mean Squared Range Error Versus Beta for SNR 27db

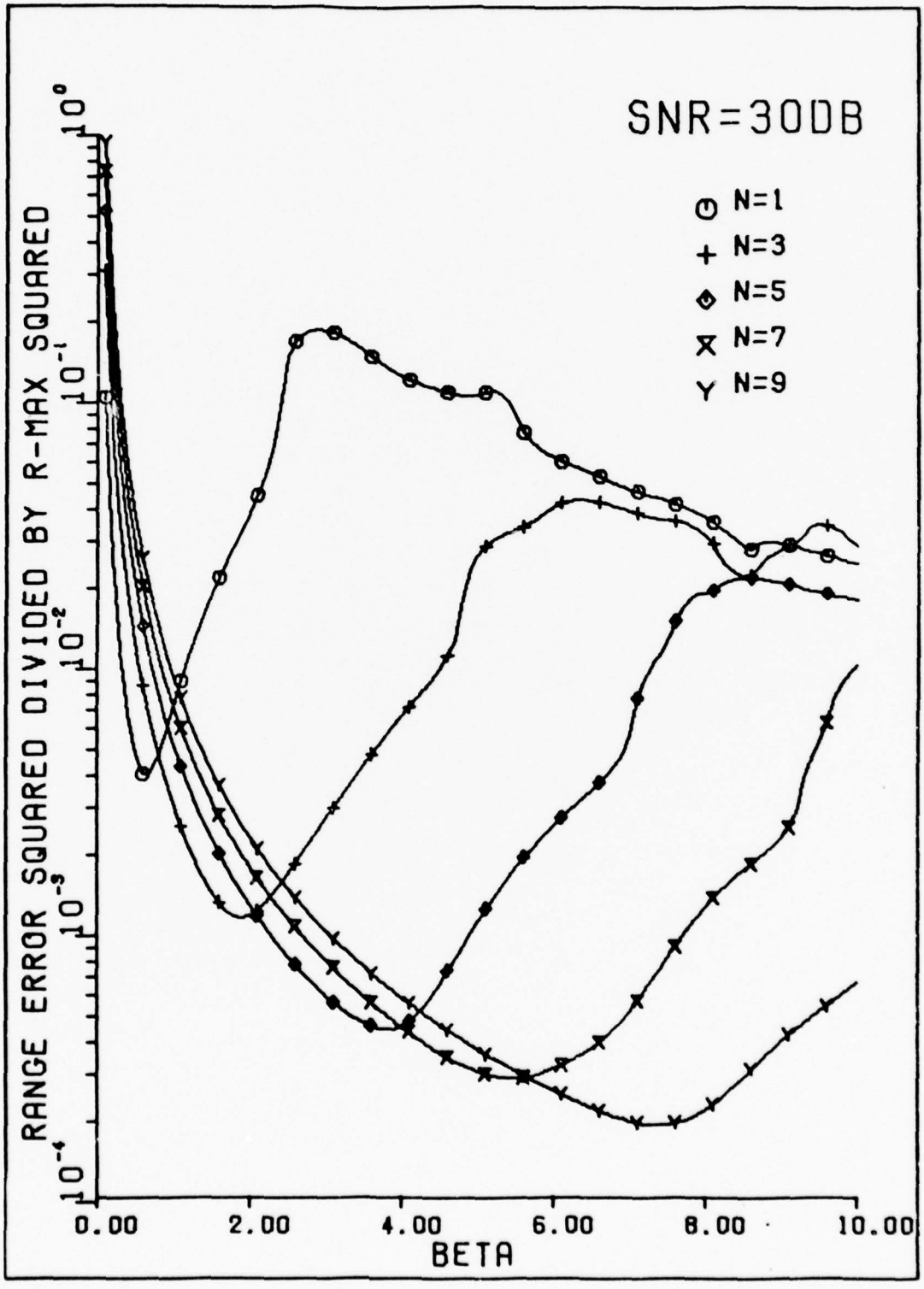

Fig. 18. Normalized Mean Squared Range Error Versus Beta for SNR = 30db

PLL exceeds the bandwidth of the spatial filter by using the expression in Eq (20). These distortion results can not be applied if the loop bandwidth is less than the spatial filter bandwidth as there will be additional distortion caused by the PLL which acts as a low pass filter. The curves show plots of the normalized mean-squared range distortion error versus β for N = 1, 3, 5, 7, and 9. The even values of N have been deleted from the plots so that the curves do not become cluttered, however, the results fall in between the odd values of N as expected. For values of N less than one, the output phase is zero and, thus, the sensor cannot resolve any objects smaller than one beamwidth. Also, the value of N is always an integer, and if the computed value of N $(1/(Xf_r))$ is not an integer, the fractional portion is truncated. The reader should be reminded that the data in the plots is in terms of relative range error, not absolute range error.

The distortion data which is plotted for various N's and SNR_{norm}'s shows some distinct trends between the sensor and terrain parameters and the range distortion error. In analyzing the distortion data r_m will always be fixed and changes in β will represent changes in the frequency of modulation, f_m. In all these curves, the tail of the curves drops off for large β and small N's because the $1/r_m^2$ normalizing term is dominant, not because the absolute range distortion error is getting smaller. As illustrated in the tail of these curves, the range distortion error does saturate because the phase error is limited to Mod 2π. As previously predicted, there is an optimum operating value of β, which is interpreted as the optimum frequency of modulation where the range error distortion is minimal. For example, if the laser line scanning sensor is used for mapping specific terrain profiles or targets the frequency

of modulation could be specifically chosen so that the minimum distortion of the range signal occurs for that target profile. The minimum distortion point decreases as the signal to noise ratio increases. The value of β for the minimum distortion point also decreases as the SNR increases. For larger values of N (larger spatial bandwidths), the minimum distortion point is at larger values of β or higher f_m. Based on this analysis of the curve trends, it is desirable to manipulate the modulation frequency so that the sensor is operating at the minimum distortion point.

The question arises as to how these plots can be used to determine distortion for a specific set of parameters. β is determined by computing $(\frac{4\pi f_m r_m}{c})$, where r_m is the peak amplitude height variation of the terrain range profile, and f_m is the frequency of modulation of the laser. N is calculated by dividing the spatial bandwidth of the beam, 1/X, by the spatial frequency of the terrain, f_r. The number of harmonics at the output of the spatial filter, N, must be an integer. If the absolute SNR is measured, then Eq (20) must be used to calculate the SNR_{norm} to use the appropriate figure. A sample calculation follows:

Sample Calculation

Given: Beam Spot Size $X = 15$ cm; Frequency of Modulation $f_m = 100$ MHz; Spatial Frequency of the Range Variations $f_r = 1.25$ cycles/m; Maximum Height Variations $r_m = 1$m; $SNR_{abs} = 20$db

$$N = \frac{1}{f_r X} \text{ (truncated to an integer value)} = 5$$

$$\beta = \frac{4\pi f_m r_m}{c} = 4.19$$

$$SNR_{norm} = SNR_{abs} + 10 \log N$$

$$SNR_{norm} = 27db$$

To find $\frac{\overline{r_e^2}}{r_m^2}$, Figure 17 is used and the curve for N = 5 with = 4.19.

$$\frac{\overline{r_e^2}}{r_m^2} = 8 \times 10^{-4}$$

$$\overline{r_e^2} = 8 \times 10^{-4}\ m^2$$

$$\sqrt{\overline{r_e^2}} \approx .03\ m$$ (or about 3% distortion of the peak range amplitude variation)

The terrain parameters f_r and r_m can be interpreted as the spatial frequency and the peak amplitude variations of the terrain range profile, respectively. For instance, if the profile of an automobile was being mapped, the peak amplitude variation that would be desirable to discern would be approximately 1.5m and the maximum spatial frequency that would be desirable to discern would be 10 cycles/m or a range variation with a period of 10 cm. This is the type of interpretation used to describe the particular target or range profile parameters.

As it is desirable to operate with minimum distortion, the optimum frequency of modulation is plotted against the normalized signal to noise ratio in Figure 19 for r_m = 1m. This single plot with one value for r_m is sufficient for describing the relation of all other r_m's because the curve scales for other values of r_m by the factor $1/r_m$. This is apparent from the previous plots where the optimum modulation frequency is determined by taking the value of β at the first minimum of the curve and dividing the value of β by $(\frac{4\pi f_m}{c})$, and noting that f_m is scaled by $1/r_m$. The upper limit on the optimum modulation frequency of 2.5×10^8 Hz in Figure 19 is the result of the largest values of β which were used in the numerical calculations, not the distortion process.

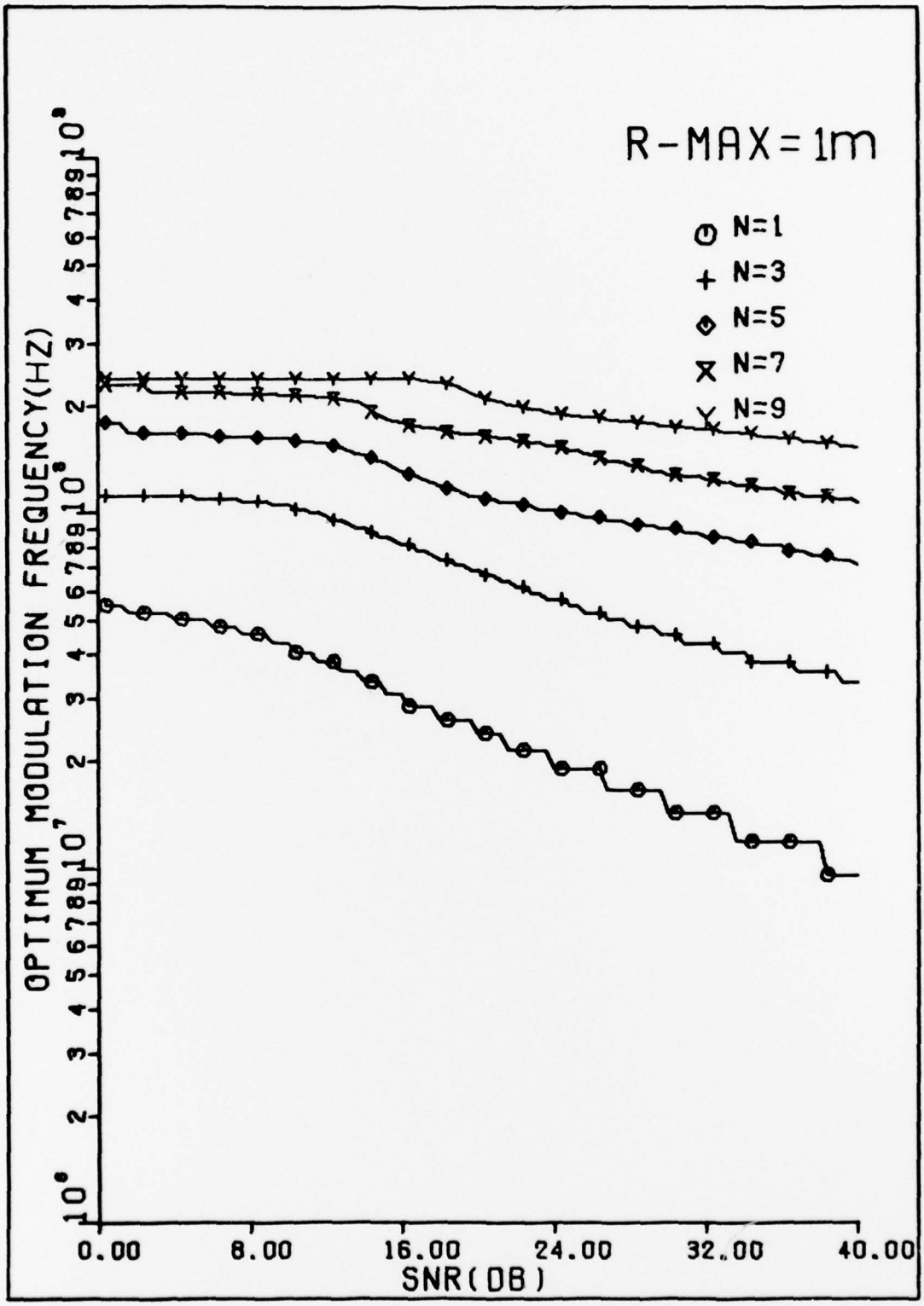

Fig. 19. Optimum Modulation Frequency Versus Signal-to-Noise Ratio for r_m = 1m

Some additional distortion calculations for some specific terrain and sensor parameters are presented in Table 1. In Table 1, various sensor and terrain parameters have been varied, and the root mean squared range distortion error has been computed from the previous curves. The resulting range distortion error is a sizeable percentage of r_m in all cases; thus, the distortion process severely limits the range accuracy of the sensor for these particular cases. In Table 1, if case 1 is compared to case 2, the spatial frequency is smaller for case 2 and the resulting rms range distortion error is smaller. If case 1 is compared to case 3, where r_m is larger in case 3, the rms range distortion error is ten times larger in case 3. A comparison of case 4 and case 5 illustrates the effect of decreasing the beam spot size. Cases 6-10 are some examples where several of the terrain and sensor parameters have been varied at the same time. Table 2 is a presentation of the same cases used in Table 1, but the optimum frequency of modulation has been picked for the sensor by using the curves presented in Figure 19. By comparing the root mean squared range error in Table 1 and Table 2, for most of the cases there are significant decreases in the range distortion error when the optimum modulation frequency is used. Even so, the range distortion still exceeds 10% of r_m in cases 1, 3, 4, 6, 7, 8, and 10, which means that a smaller beam spot size will be the only way to reduce the distortion any further.

If the sensor is used in a forward looking configuration as shown in Figure 20, then the distortion results can be extended to evaluate its range distortion performance when the system is used at low grazing angles. Both the beamwidth and the range amplitude variations which are seen by the sensor are modified from their original definitions. In Eq

Table 1. Some Specific Range Distortion Calculations

Case #	Beam Size X (m)	Freq of Modu f_m(Hz)	SNR_{abs} (db)	f_r (c/m)	r_m (m)	N	β	SNR_{norm} (db)	$\sqrt{r_e^2}$ (m)
1	.15	1×10^8	20	6	.24	1	1.0	20	.03
2	.15	1×10^8	20	1.25	.24	5	1.0	27	.02
3	.15	1×10^8	20	6	1.0	1	4.19	20	.35
4	.15	1×10^8	20	6	2.0	1	8.38	20	.36
5	.03	1×10^8	20	6	2.0	5	8.38	27	.30
6	.15	1×10^7	10	6	5.0	1	2.09	10	1.32
7	1.0	1×10^7	10	1	10.0	1	4.19	10	3.5
8	1.0	1×10^8	20	1	1.0	1	4.19	20	.35
9	1.0	1×10^9	30	1	.15	1	6.28	30	.036
10	1.0	5×10^8	20	1	.4	1	8.38	20	.075

Table 2. Some Range Distortion Calculations with Minimum Distortion

Case #	Beam Size X (m)	SNR_{abs} (db)	SNR_{norm} (db)	f_r (c/m)	r_m (m)	N	Optimum f_m (Hz)	β	$\sqrt{\overline{r_e^2}}$ (m)
1	.15	20	20	6	.24	1	1.04×10^8	1.05	.03
2	.15	20	27	1.25	.24	5	3.96×10^8	3.98	.007
3	.15	20	20	6	1.0	1	2.5×10^7	1.05	.13
4	.15	20	20	6	2.0	1	1.25×10^7	1.05	.27
5	.03	20	27	6	2.0	5	4.75×10^7	3.98	.06
6	.15	10	10	6	5.0	1	8.4×10^8	1.76	1.28
7	1.0	10	10	1	10.0	1	4.2×10^8	1.76	2.6
8	1.0	20	20	1	1.0	1	2.5×10^7	1.05	.13
9	1.0	30	30	1	.15	1	1.0×10^8	.628	.01
10	1.0	20	20	1	.4	1	6.25×10^7	1.05	.05

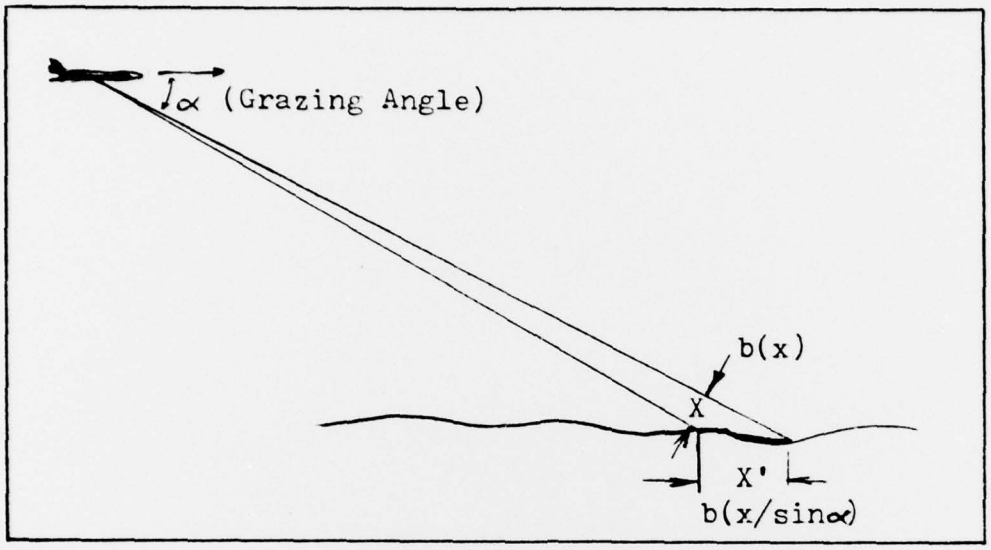

Fig. 20. Forward Looking Configuration for the Laser Terrain Mapping Sensor

(21) the expressions for the new r_m and X are presented.

$$X' = X/\sin\alpha \tag{21a}$$

$$r_m' = \sqrt{(X')^2 - (r_m \sin\alpha)^2} \tag{21b}$$

This is not a complete description of the forward looking configuration as the filter function would also have to be modified, but it is reasonable for obtaining results for design calculations to check the feasibility. A sample calculation for the forward looking configuration follows:

Sample Calculation for Forward Looking Configuration

Given: $X = .15$ m $\quad f_r = 1.25$ cycles/m

$f_m = 1 \times 10^8$ Hz $\quad SNR_{abs} = 20$db

$r_m = .24$ m $\quad \alpha = 15°$

Calculated: $X' = .58$ m $\quad r_m' = .58$ m $\quad \beta = 2.43$

$N = 7$ $\quad SNR_{norm} = 28.5$db (Need to interpolate between Figures 17 and 18)

$\frac{\overline{r_e^2}}{r_m^2} = 1.9 \times 10^{-3}$ and $\sqrt{\overline{r_e^2}} = .025$ m

IV. Conclusions and Recommendations

The basis of this theoretical study was to analyze the spatial filtering distortion effects on the performance of the laser line scanning sensor. Some specific distortion results were presented which showed the interaction between the terrain characteristics and the sensor parameters. From this analysis and the distortion results, several conclusions and recommendations can be made.

Conclusions

This study began with an examination of a one dimensional spatial filtering model. An attempt was made to model the terrain range and reflectivity as Gaussian Random Processes. This model of the terrain only served the spatial filtering analysis by describing the conditions for no distortion. Next, a detailed examination of the distortion effects was made to determine what simplifications were necessary to make the analysis more tractable. Specifically, two approaches were modeled, linearization of the phase modulated range signal and the case when the terrain height profile was constant. In addition, a model for sampling receivers as applied to pulse types of modulation for the laser was analyzed.

The next step in the analysis was to obtain some distortion results which were useful in determining the interaction between the sensor and terrain parameters and their effect on the distortion. First, the output of the spatial filter was represented in terms of the input terrain parameters. Analytically, this solution was not very tractable and once again simplifications were required. One simplification involved the removal of the reflectivity dependence which reduced the complexity of

the analysis. But the primary approach which was ensued, was to model the terrain height profile as a single sinusoid and to assume that the reflectivity was constant so that the received signal was the phase modulated terrain height profile. Then, this phase modulated signal was filtered by an ideal low pass filter which represented the effects of the spatial filter (finite beam size). In addition, another distortion process, caused by the receiver noise in the phase tracking circuitry, was modeled. Using the two distortion processes, the total range distortion error was calculated for various terrain and sensor parameters, and was presented as set of plots. Some specific distortion calculations were made. From the range distortion error curves and calculations, several trends in the data were observed. Given the maximum height variation of the terrain, there was an optimum frequency of modulation for the laser where the range distortion error was minimized. This minimum distortion point was found to be dependent upon the SNR, the spatial frequency of the terrain, the beam spot size, and the maximum height variations of the terrain. The optimum frequency of modulation decreased when the SNR increased, and the range distortion error at this point decreased. In addition, when the beam spot size was reduced or the bandwidth of the spatial filter was increased, the optimum frequency of modulation decreased, and the range distortion error at this point decreased. The range distortion error increased when the spatial frequency of the terrain range variations was increased. Based on these trends and the distortion data, it was determined that the sensor performance could be improved by optimizing the frequency of modulation of the laser for a particular set of terrain characteristics and sensor parameters. The data was restructured as a plot of the frequency of modula-

tion of the laser for minimum distortion versus the signal-to-noise ratio. Finally, an extension of the distortion calculations was applied to the forward looking configuration of the terrain mapping laser sensor.

The following conclusions can be drawn from this thesis:

1. The performance of the laser line scanning sensor can be improved by removing the reflectivity dependence.

2. For pulsed types of scanner modulation, it was determined that the output of the spatial filter was bandlimited by the bandwidth of the spatial filter.

3. Throughout the analysis no information was available about terrain features which were smaller than the beam spot size.

4. The performance of the terrain mapping sensor could be improved by selecting the optimum modulation frequency for a given set of terrain and sensor parameters.

Recommendations

Several recommendations resulted from this study and all of them apply to follow-on studies of the spatial filtering distortion problem. First, the spatial filtering distortion should be re-examined and recalculated for other periodic and nonperiodic range functions using other distortion measures and calculation techniques from different sources (which are included in the Bibliography). The distortion range error should be recalculated for a Gaussian shaped filter which more closely represents the spatial filter. Furthermore, the results which were obtained do not apply to time domain processing receivers where all the harmonics of the periodic modulation are detected. For these calculations, Fast Fourier Transform techniques will probably serve as a useful numerical technique, and could be utilized to analyze specific height profiles of

the terrain. Finally, the forward looking configuration of the sensor needs to be re-analyzed in depth.

Bibliography

1. Kingston, R. H. "Airborne Surveillance and Reconnaissance." AGARD Groupe Consultatif Pour la Recherche et le Developpement Aerospatial, Evaluation of the Potential Benefit to the Aeronautical Field from Laser Technology: AGARDographic No. 195: 6-1 to 6-3 (December 1974). AGARD-AG-195.

2. Robinson, S. R. Design Considerations for a Laser Three Dimensional Target Sensor. Draft Report, Department of Electrical Engineering, Air Force Institute of Technology, Wright-Patterson AFB, Ohio 45433, June 1976.

3. Chapuran, R. C. An Analysis of Modulation Techniques for the Simultaneous Measurement of Range and Reflectance Information by an Airborne Laser Scanner. Master Thesis, Air Force Institute of Technology, Wright-Patterson AFB, Ohio 45433, December 1976, GE/EE/76-18. AD-A035291/4WH.

4. Robinson, S. R. and R. S. Reinman. "Bandwidth Considerations for a Modulated Scanner." Department of Electrical Engineering, Air Force Institute of Technology, Wright-Patterson AFB, Ohio 45433.

5. VanTrees, Harry L. Detection, Estimation, and Modulation Theory, Part II: Nonlinear Modulation Theory. New York: John Wiley & Sons, Inc., 1971.

6. Middleton, David L. Introduction to Statistical Communication Theory. New York: McGraw-Hill, 1960.

7. DeRosa, Joseph K. "The Spectral Density of a Sinusoid Phase Modulated by a Gaussian-Filtered Gaussian Process." IEEE Transactions on Communications; 24: 935-938, August 1976.

8. Giacoletto, L. J. "Generalized Theory of Multitone Amplitude and Frequency Modulation." Proceedings of the IRE, 35: 680-693, July 1947.

9. Williams, O.E., Jr. "Comparison of Bedrosian-Rice and Curson-Fry Methods for Calculating Angle Modulation Distortion." IEEE Transactions on Communications, 21: 971-975, August 1973.

10. Bedrosian, E. and S. O. Rice. "Distortion and Crosstalk of Linearly Filtered, Angle-Modulated Signals." Proceedings IEEE, 56: 2-13, January 1968.

11. Tuê, Huynh Huu. "A New Approach to Computing Distortion of an FM Single-Tone Modulated Signal Due to Ideal Filtering." IEEE Transactions on Communications, 24: 1317-1321, December 1976.

12. Jeruchim, Michel C. "Interference in Angle-Modulated Systems with Predetection Filtering." IEEE Transactions on Communications, 28: 723-726, October 1971.

13. Shimbo, Osamn and Chun Loo. "Digital Computation of FM Distortion Due to Bandpass Filters." IEEE Transactions on Communications, 17: 571-574, October 1969.

14. Plotkin, Sheldon C. "FM Bandwidth as a Function of Distortion and Modulation Index." IEEE Transactions on Communications, 15: 467-470, June 1967.

15. Ruthroff, Clyde L. "Computation of FM Distortion in Linear Networks for Bandlimited Periodic Signals." BSTJ, 47: 1043-1063, July-August 1968.

VITA

William D. Strautman attended the University of Cincinnati and received a B.S.E.E. degree in 1973. After being commissioned in the USAF, he served as a test engineer at Rome Air Development Center, Griffiss AFB, for approximately three years. He is currently enrolled in the Air Force Institute of Technology's Electro-Optics program which leads to an MSEE degree.

UNCLASSIFIED

SECURITY CLASSIFICATION OF THIS PAGE (When Data Entered)

REPORT DOCUMENTATION PAGE		READ INSTRUCTIONS BEFORE COMPLETING FORM
1. REPORT NUMBER AFIT/GEO/EE/77-6	2. GOVT ACCESSION NO.	3. RECIPIENT'S CATALOG NUMBER
4. TITLE (and Subtitle) SPATIAL FILTERING DESIGN CONSIDERATIONS FOR A LASER LINE SCANNING SENSOR		5. TYPE OF REPORT & PERIOD COVERED MS Thesis 6. PERFORMING ORG. REPORT NUMBER
7. AUTHOR(s) William D. Strautman Captain, USAF		8. CONTRACT OR GRANT NUMBER(s)
9. PERFORMING ORGANIZATION NAME AND ADDRESS Air Force Institute of Technology (AFIT/EN) Wright-Patterson AFB, Ohio 45433		10. PROGRAM ELEMENT, PROJECT, TASK AREA & WORK UNIT NUMBERS
11. CONTROLLING OFFICE NAME AND ADDRESS Electro-Optics and Reconnaissance Branch Air Force Avionics Laboratory (AFAL/RWI) Wright-Patterson AFB, Ohio 45433		12. REPORT DATE December 1977 13. NUMBER OF PAGES 58
14. MONITORING AGENCY NAME & ADDRESS (if different from Controlling Office)		15. SECURITY CLASS. (of this report) Unclassified 15a. DECLASSIFICATION/DOWNGRADING SCHEDULE

16. DISTRIBUTION STATEMENT (of this Report)

Approved for public release; distribution unlimited.

17. DISTRIBUTION STATEMENT (of the abstract entered in Block 20, if different from Report)

18. SUPPLEMENTARY NOTES

Approved for public release; IAW AFR 190-17

JERRAL F. GUESS, Captain, USAF
Director of Information

19. KEY WORDS (Continue on reverse side if necessary and identify by block number)

Terrain Mapping
Laser Line Scanner
Active Laser Sensors
Spatial Filtering

20. ABSTRACT (Continue on reverse side if necessary and identify by block number)

The performance of an airborne laser terrain mapper, which collects slant range and reflectance data simultaneously, is determined in part by the spatial filtering effects of the finite laser beam spot size. An analysis of the spatial filtering effects and the resulting distortion of the terrain profile slant range to the aircraft is made to interpret the interaction between the terrain characteristics and the resulting laser line scan information. Emphasis is placed on the range interactions. In particular, the terrain height profile is modeled as a single sinusoid in one spatial dimension with constant reflectivity.

DD FORM 1 JAN 73 1473 EDITION OF 1 NOV 65 IS OBSOLETE

UNCLASSIFIED

SECURITY CLASSIFICATION OF THIS PAGE (When Data Entered)

Block 20. Abstract. (Continued)

The laser transmitter is sinusoidally intensity modulated, so that the received signal is subcarrier phase modulated by the terrain height profile. This phase modulated signal is low pass filtered to represent the effects of the spatial filter. Numerical analysis is utilized to evaluate this nonlinear filtering problem and to examine the range error in terms of the maximum range height variations. The resulting mean-squared range distortion error is added to the range squared distortion error originating from the receiver noise in the Phase Locked Loop phase tracking circuit. The distortion due to spatial filtering is shown to increase with the laser modulation frequency while the errors due to detection noise decrease with frequency. Thus, the performance of the receiver can be optimized according to the terrain maximum range height variations and the desired resolution by designing the properly sized optics and choosing an optimum frequency of modulation. In addition, the general spatial filtering model is extended to evaluate the performance of a forward looking laser terrain mapper using low grazing angles.